Applications of Laser Ablation–Inductively Coupled Plasma–Mass Spectrometry (LA-ICP-MS) to Gemology

Ahmadjan Abduriyim and Hiroshi Kitawaki

Laser ablation–inductively coupled plasma–mass spectrometry (LA-ICP-MS) is an important technique for quantitative chemical analysis. The authors have applied this minimally destructive technique to gemology to take advantage of its high spatial resolution, rapid and direct analysis of gemstones (whether loose or mounted), and precise measurement of a wide range of elements—even in ultra-trace amounts. This article summarizes LA-ICP-MS principles and describes the successful application of this technique to detecting beryllium diffusion treatment in corundum and identifying the geographic origin of emeralds. LA-ICP-MS is significantly less expensive than SIMS and more sensitive than LIBS, which is the least costly of the three instruments.

In recent years, gemologists worldwide have faced a variety of new treatments, synthetics and simulants, and gem sources that have caused confusion in the trade. Several techniques—including UV-visible, infrared, and Raman spectral analysis—have been employed to solve some of these problems. However, each of these techniques has limitations, and even in combination they have not been entirely successful in addressing all of these challenges. Now, chemical analysis by laser ablation–inductively coupled plasma–mass spectrometry (LA-ICP-MS) has emerged as a powerful tool for gemologists.

ICP-MS has been used for decades to chemically characterize materials, but historically this technique has required dissolving solid samples in strong acids prior to analysis. The use of laser ablation with ICP-MS was developed by Gray (1985) and became commercially available in the early- to mid-1990s. Combined with the development of extremely sensitive mass spectrometers, laser ablation allowed ICP-MS to be used on gemstones with minimal damage, since the laser vaporizes only a microscopic amount of the sample for analysis. Additional advantages include a high spatial resolution (just a few micrometers), low detection limits, and high precision and accuracy. This technique is also particularly attractive to scientists who want to study micro-spatial distributions of trace elements and isotopic compositions, from light (helium) to heavy (uranium). In addition, the analysis is rapid and no sample preparation is required. As a result, LA-ICP-MS has become one of the most exciting instruments in gemology, geology, and materials science.

LA-ICP-MS analyses provide quantitative data for major, minor, and trace elements in the analyzed samples, from which variation diagrams and "chemical element fingerprints" can be established. Such fingerprinting can reveal differences between samples that may be attributed to the geographic origin of

See end of article for About the Authors and Acknowledgments.
Gems & Gemology, Vol. 42, No. 2, pp. 98–118.

Figure 1. In late 2001, substantial numbers of beryllium diffusion–treated sapphires entered the gem trade, spurring a need for proper identification. Shown here are a collection of loose and mounted beryllium-diffused sapphires (the mounted stones include some untreated sapphires). The bracelet and earrings are courtesy of Michael Couch & Assocs.; the loose sapphires are courtesy of Deepam Inc. and Robert E. Kane. Photo by Harold & Erica Van Pelt.

the sample or subsequent treatment. An introduction to the potential use of this method in gemology was reported by Günther and Kane (1999a,b). Due to the high cost of the instrumentation and the microdestructive nature of the method, gemologists were slow to explore its full range of applications. At this time, however, the Gemmological Association of All Japan (GAAJ, in Tokyo), Gemological Institute of America (GIA, in Carlsbad), Central Gem Laboratory (CGL, in Tokyo), and Tiffany & Co.'s Merchandise and Testing Laboratory (in New Jersey) all have LA-ICP-MS systems for gemstone analysis (as well as other applications, such as metals testing). Other gemological labs use LA-ICP-MS systems at nearby universities. For example, the Gübelin Gem Lab (Lucerne, Switzerland), the GRS Gemresearch Swisslab (Lucerne), and the SSEF Swiss Gemmological Institute (Basel) have access to the LA-ICP-MS facilities at the Swiss Federal Institute of Technology (ETH) Laboratory in Zurich.

LA-ICP-MS has been applied to a variety of topics in earth sciences (see, e.g., Hirata and Nesbitt, 1995; Jeffries et al., 1995; Jackson et al., 2001; Norman, 2001) and archeology (e.g., Pollard and Heron, 1996; Devos et al., 2000; Tykot, 2002). However, publications on the application of LA-ICP-MS to gem materials were uncommon until relatively recently (Watling et al., 1995; Günther and Kane, 1999a,b; Guillong and Günther, 2001; Rankin et al., 2003; Saminpanya et al., 2003; Wang et al., 2003; Abduriyim and Kitawaki, 2006).

In this article, we will examine two areas in which LA-ICP-MS can be particularly useful: detecting new treatments and determining the geographic origin of gemstones (using the specific example of emeralds).

Detection of New Treatments. Toward the end of 2001, unprecedented amounts of saturated orange-pink to pinkish orange sapphires (the so-called padparadscha colors), as well as yellow sapphires, became widely available on the worldwide jewelry market (Scarratt, 2002; Shida et al., 2002; see figure 1). Many studies subsequently revealed that beryllium (Be) had been diffused into the sapphires at high temperatures, with the Be originating from chrysoberyl (see, e.g., Emmett et al., 2003, and references cited therein). Because beryllium is a "light" (i.e., low atomic weight) element, trace levels of Be cannot be detected by most analytical techniques, including energy-dispersive X-ray fluorescence (EDXRF), energy-dispersive spectroscopy with a scanning electron microscope (SEM-EDS), and, in some cases, electron-microprobe analysis (EMPA). Secondary ion mass spectrometry (SIMS) has proved successful in detecting trace amounts of Be, but analyses are extraordinarily expensive (see, e.g., Emmett et al., 2003; Novak et al., 2004). For this reason, the present authors focused their attention on LA-ICP-MS. Since May 2003, GAAJ has offered an identification service for Be-diffused heat-treated corundum, using LA-ICP-MS. Recently, a less expensive instrument, laser-induced breakdown

spectroscopy (LIBS), has been applied to this problem, but it has some limitations, as discussed below.

Geographic Origin Determination. Geographic origin is an important consideration for many gem materials in some markets. Within Japan in particular, geographic origin may be a critical factor in the sale of major gems such as corundum, emerald, tourmaline, alexandrite, and opal. However, without reliable and detailed analytical data, determination of origin may be difficult, if not impossible. Even the most experienced laboratories regard origin determinations as opinions based largely on the experience, literature, and/or data collected by that laboratory. Thus, there is a need for origin determinations based on a more rigorous scientific foundation.

BACKGROUND

Chemical Analysis of Gem Materials. EDXRF and SEM-EDS are the standard methods used in gemological laboratories for the nondestructive qualitative (and possibly quantitative) chemical analysis of gem materials (see, e.g., Stockton and Manson, 1981; Stern and Hänni, 1982; Muhlmeister et al., 1998). EDXRF is capable of measuring the chemical composition of a gemstone in a matter of minutes, by detecting the energy of emitted X-rays that are produced when the sample is exposed to an X-ray beam. With SEM-EDS, an electron beam scans across the specimen's surface, producing signals from secondary or backscattered electrons that can be used to produce a high-resolution image. In addition, X-rays emitted from the sample can reveal its chemical composition. Using an attachment for energy-dispersive spectroscopy, a more precise chemical composition can be obtained with the SEM at high spatial resolution. Although both EDXRF and SEM-EDS are limited in their detection and measurement of light elements, when combined with other analytical methods such as UV-Vis spectroscopy, they can identify some trace elements that provide useful information on the geologic occurrence, geographic origin, and causes of color in gem materials.

EMPA is another well-established method being used in gemology (Dunn, 1977). This technique uses a high-energy focused beam of electrons to generate X-rays characteristic of the elements within a sample. It can provide quantitative analyses of elements ranging from beryllium (in some cases) to uranium, at levels as low as 100 parts per million (ppm or µg/g, which are fractional weights). Thus far, this is the only fully quantitative technique that is nondestructive. Unfortunately, EMPA is not useful for analyzing beryllium in diffused corundum, since Be is present in amounts that are below the detection limit of the instrument.

SIMS is a powerful micro-destructive technique for chemical analysis of a wide variety of solid materials (Benninghoven et al., 1987). A beam of primary ions such as oxygen or argon is focused on the sample, causing a very small amount of the surface to be sputtered. A portion of the sputtered atoms are ionized and extracted using an electrical field. The ionized atoms are then filtered according to their energy and mass by an electrostatic sector and a magnetic field, at which point they go to a mass spectrometer for isotopic analysis. This technique can provide sensitivities near parts per billion (ppb or ng/g) for all elements from hydrogen to uranium. However, it is only available in some universities and research laboratories due to its high cost and sophisticated operating requirements.

LIBS can detect a full range of major, minor, and trace elements simultaneously (see, e.g., García-Ayuso et al., 2002), and its low cost and easy operation have attracted the interest of several gem laboratories. A single-pulse high-energy Nd:YAG 1064 nm laser is used to vaporize a microscopic area of a sample at high temperature (i.e., >5000°C–10,000°C), and the sputtered particles are broken down into a mixture of atoms, ions, and electrons. After the laser pulse has ended, excited electrons in the atoms drop down to a low energy level and discharge light. By detecting the wavelength and strength of this emission with a high-resolution fiber-optic spectrometer, optical emission spectra can be generated that may then be converted to qualitative and semiquantitative chemical data. However, precise quantitative analyses cannot be obtained with this technique (Krzemnicki et al., 2004; Themelis, 2004).

LA-ICP-MS Instrumentation. The LA-ICP-MS analysis process can be thought of in two main parts: sampling (i.e., laser ablation and ionization in a plasma) and mass spectrometry. While mass spectrometry has been well developed for many decades, the sampling techniques of laser ablation and inductively coupled plasma were developed more recently.

Mass Spectrometry. Following J. J. Thomson's use of electromagnetic fields to separate ions for analysis (Thomson, 1911), scientists such as Dempster (1918), Aston (1919), and Stephens (1946) developed this technique into what it is today, a highly sensitive

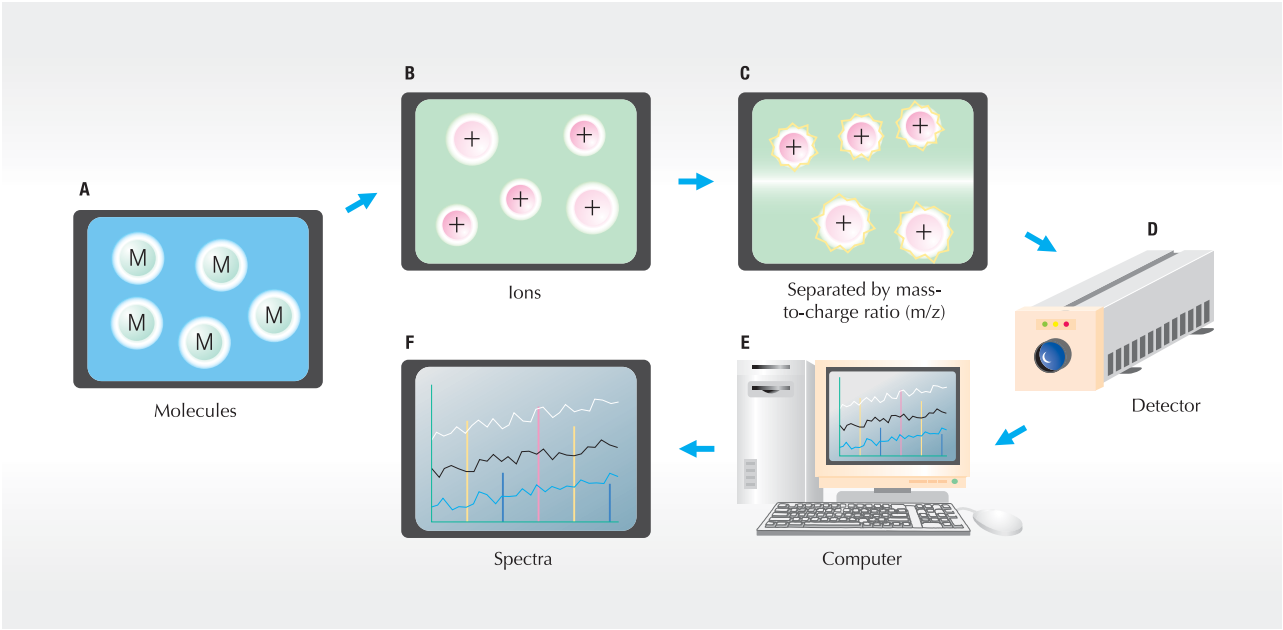

Figure 2. This chart shows how a mass spectrum is obtained from a sample. Gaseous molecules of the sample (A) are ionized to form gaseous ions (B). The ions are separated according to their mass-to-charge ratio when they pass through a mass analyzer (C) to the detector (D). A computer (E) transforms the signal from each element into a spectrum, which is displayed on the screen (F).

method capable of analyzing both chemical elements and small organic molecules. Early mass spectrometers required that the sample be in a gaseous state, but developments over time have expanded the applicability of mass spectrometry to include solutions and solids. A mass spectrometer is an instrument that measures the masses of elements or molecules of chemical compounds by separating charged particles according to their mass-to-charge ratio (m/z; in most cases, the value of z = +1). The sample is ionized and the ions are electrostatically directed into a mass analyzer, where they are separated according to their m/z ratio and then sent to a detector (figure 2). A spectrum is then generated that represents the masses of components of a sample.

The most popular mass spectrometer used in ICP-MS is the quadrupole mass analyzer (figure 3), which consists of four parallel metal rods arranged in a square. Each pair of opposite rods has a combined AC and DC electrical potential. When the DC and AC voltages are set to certain values, only ions with a specific m/z ratio are able to continue on a path between the rods. By sequentially selecting many combinations of voltages, the technician can detect an array of different ions. Semi-quantitative measurements of the mass spectrum or isotope ratios are obtained by measuring the intensities of the ions passing through the quadrupole mass analyzer as the voltages on the rods are varied.

Inductively Coupled Plasma. In the 1980s, inductively coupled plasma at atmospheric pressure was developed as a technique for ionizing samples. The sample (in solution or vaporized using a laser ablation system) is conveyed in a flow of argon gas into a torch that is inductively heated to approximately 10,000°C. At this temperature almost all matter in the sample is atomized and ionized, forming a plasma that provides a rich source of both excited and ionized atoms (Jarvis et al., 1992). With the combination of ICP and MS technologies, rapid quantitative elemental analysis with high accuracy and low detection limits became possible.

Laser Ablation. The combination of laser ablation with ICP-MS has been widely used for multi-elemental determination and *in situ* isotopic analysis of solid materials (Gray, 1985; Arrowsmith, 1987). In the laser ablation process, the sample is placed in the ablation cell (which does not need to be under vacuum), and a minute portion of its surface is vaporized using a pulsed high-energy laser beam that is directed through the objective lens of a modified petrographic microscope. The surface of the sample is viewed with a charge-coupled device (CCD) camera mounted on the microscope, allowing for precise location of the laser spot. The laser pulses cause energetic atoms, ions, molecules, and solid particles to be ejected from the target, and these ablated aerosols are transported in argon or helium gas to the

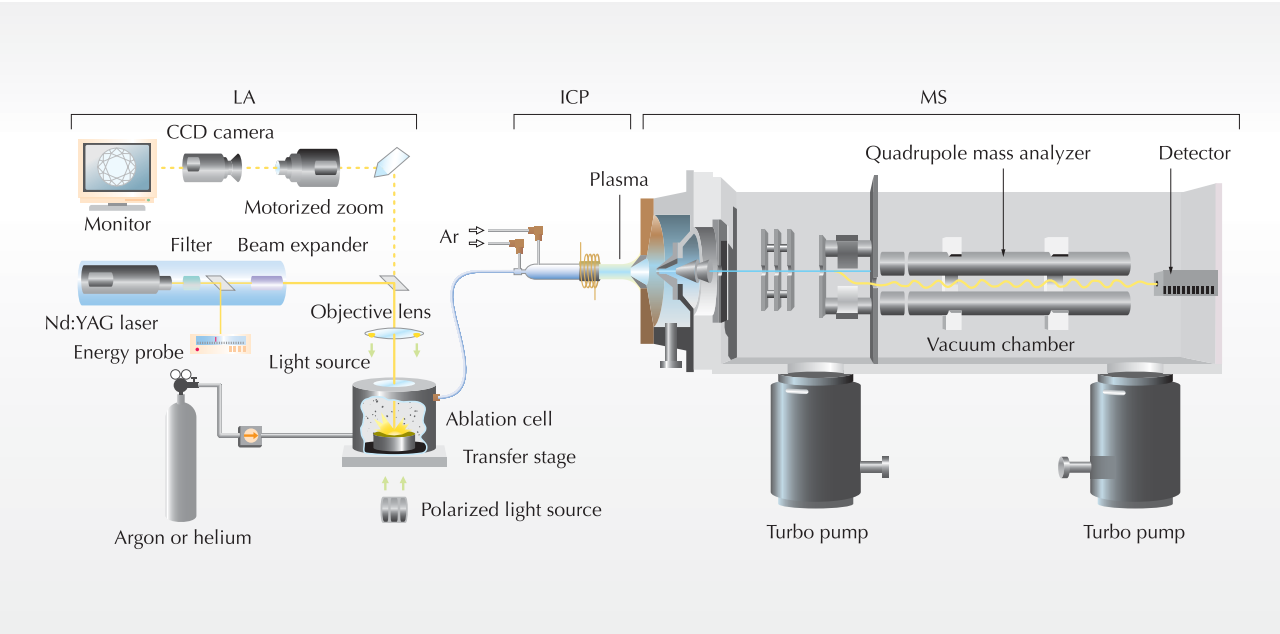

Figure 3. This schematic diagram shows the components of a 213 nm Nd:YAG laser ablation system combined with a quadrupole ICP-MS instrument. The sample is placed in the ablation cell and the laser beam is focused onto the sample with the help of a CCD camera. The ablated material forms an aerosol, which is transported by an argon or helium carrier gas to the plasma of the ICP-MS. At the ICP, laser-ablated particles are vaporized and ionized. The ions are extracted by the vacuum interface and guided into the mass analyzer, where they are separated by their mass-to-charge ratio and finally detected.

plasma of the ICP-MS. Helium is typically used as the carrier gas in the sample cell, and is combined with Ar in the tubing that leads to the ICP. During the ablation process, less material is left around the laser spot crater when using He as compared to Ar, so more of the sample can be transferred to the ICP, leading to a higher-intensity, more stable signal (Günther and Heinrich, 1999). Two types of laser have been widely used for ablating minerals or glassy materials: (1) an argon fluoride (ArF) excimer laser with a wavelength of 193 nm (Loucks et al., 1995; Günther et al., 1997; Horn et al., 2000), and (2) a Nd:YAG 1064 nm (infrared) laser that is frequency-multiplied to UV wavelengths (fourth harmonic at 266 nm and fifth harmonic at 213 nm; Jenner et al., 1993; Jeffries et al., 1998).

Data Quality Considerations. A mass spectrum consists of a series of peaks representing the distribution of components (atoms or molecules) by mass-to-charge ratio. The relative intensities of the various isotopes in the spectrum provide a semi-quantitative chemical analysis (Tye et al., 2004). To produce quantitative data, the analysis of a sample must be calibrated against an external standard of known composition, that is, by measuring the signals for the elements of interest in the sample and comparing them to the signals from a standard with known concentrations of those elements. Several calibration strategies have been developed for quantification of LA-ICP-MS analyses, including those using solid standards (glass, ceramic, cement, and metals) and those using standard solutions (Kanicky and Mermet, 1999). In general, the use of matrix-matched standards (e.g., a corundum standard for analyzing sapphires) is advantageous, because the ablation behavior will be similar for both the standard and the sample. However, in many cases this approach is limited by a lack of suitable materials. For example, NIST (National Institute of Standards and Technology) glass is widely used as an external standard for successfully analyzing the trace-element contents of silicates and carbonates. However, the matrix of simple oxide minerals (e.g., corundum) is much different from the NIST glass. Variation in these matrices can give rise to inconsistencies in ionization efficiency, which will create differences in the signal of a given element in those materials (even if they contain identical concentrations of the element).

To obtain accurate quantitative chemical data for gem corundum, the external standard should consist of a well-characterized homogenous sample of ultra-pure synthetic corundum that has been

doped with the element(s) of interest. However, if such a standard is not available, an internal element standard may be used to correct the analyzed signals. In this procedure, the concentration of Al in the sample is measured using another quantitative technique, such as EMPA. Calibration for other elements in the sample can then be achieved by comparing the LA-ICP-MS signal for Al obtained from an external NIST glass standard to that obtained from the specimen.

MATERIALS AND METHODS

For our investigations of beryllium diffusion–treated corundum, we used LA-ICP-MS to analyze a total of 121 faceted natural and synthetic rubies and sapphires: 21 were unheated, 19 were subjected to traditional heat treatment, and 81 were treated with Be diffusion and then repolished (table 1). Some of the stones treated by Be diffusion were analyzed before and after treatment to confirm that Be was diffused by the process; these samples included four colorless sapphires and four rubies, as well as eight colorless Verneuil synthetic sapphires and two pink flux-grown synthetic sapphires. At the request of the authors, treaters in Thailand heated the stones in a crucible together with powdered chrysoberyl to over 1800°C in an oxidizing atmosphere (for 22 hours in Bangkok and more than 10 hours in Chanthaburi). Samples SCL001, SCL003, VCS001, and VCS005 were cut in half after Be-diffusion treatment and eight point analyses were performed by LA-ICP-MS on the cut cross-section of each sample. In addition, sample MPd-H1 was used for both LA-ICP-MS and SIMS analyses, with six point analyses across the cut cross-section.

The emeralds analyzed by LA-ICP-MS for geographic origin investigations consisted of 29 faceted Brazilian stones and 82 parallel-polished slabs, cabochons, and faceted samples from Colombia, Nigeria, Zambia, Zimbabwe, Pakistan, and Afghanistan (table 2). Of the latter samples, 50 parallel-polished slabs were supplied by Dr. Dietmar Schwarz; these emeralds were purchased or collected directly from the mine areas. The authors acquired the other samples at the Tokyo and Tucson gem fairs. The samples covered the color range from light green to deep green. FTIR and Raman spectroscopic analyses showed that, with only a few exceptions, the emeralds were not filled with oil or resin. LA-ICP-MS data for 26 elements were obtained from three different areas on each sample. Averaged data were used for the ranges that are reported in table 2.

The LA-ICP-MS analyses were obtained with a New Wave Research laser ablation system (using a Merchantek UP-213A/F laser) combined with a quadrupole ICP-MS instrument from Agilent (7500a series). The operating conditions of the LA-ICP-MS used for this study are indicated in table 3. Analytical sensitivity improves as the amount of vaporized sample increases, and our research showed that it was advantageous to inscribe our logo "GAAJ" on the girdle of all specimens during the laser ablation process (figure 4). This allowed us to obtain good sensitivity for light elements with the least "damage" to the sample. When testing for Be-diffused corundum, care was taken to avoid analyzing areas that might contain interfering inclusions. This very small inscription proves the analysis has been conducted and does not affect the beauty of a gemstone. As with laser inscriptions that are currently performed on diamonds, the LA-ICP-MS laser logo is barely visible with a 10× loupe.

Calibration was done using NIST SRM 612 multi-element glass (Pearce et al., 1997), with Al as the internal element standard (based on an average Al_2O_3 concentration of 99.00%, determined by EMPA) for corundum analyses; the same NIST standard was used for emerald calibration.

We monitored the signals of selected isotopes in the corundum and emerald samples, and the concentrations of some of these elements in the samples were calculated (see table 3). "Blank" samples of carrier gas were repeatedly analyzed (10 times) at regular intervals to determine the detection limit of each element (table 4). The higher background counts for Na, Si, Ca, and Fe were related to mass interference from the sum of various elements in the air within the instrument—^{28}Si ($^{12}C^{16}O$), ^{29}Si ($^{12}C^{16}O^{1}H$), ^{44}Ca ($^{12}C^{16}O_2$), ^{56}Fe ($^{40}Ar^{16}O$), ^{57}Fe ($^{40}Ar^{16}O^{1}H$)—and/or contamination of the system with debris from the NIST SRM 612 calcium silicate glass where, for example, a silicon ion from the glass might be misidentified as a corundum impurity—^{23}Na (^{23}Na), ^{28}Si (^{28}Si), ^{43}Ca (^{43}Ca or $^{27}Al^{16}O$), ^{44}Ca ($^{28}Si^{16}O$), ^{56}Fe ($^{40}Ca^{16}O$ or $^{28}Si^{28}Si$)—before the measurements were made. Due to these possible interference problems, we monitored two isotopes each of Si, Ca, and Fe. Concentration levels in this article are described as *trace* elements (<10,000 ppm or <1 wt.%), *minor* elements (<10 wt.% or <100,000 ppm), and *major* elements. To facilitate comparison with the literature, some trace-element values have been

TABLE 1. Corundum samples analyzed by LA-ICP-MS for Be-diffusion investigations.[a]

Sample nos.	No. of samples	Description	Origin	Weight (ct)	Be (ppm)		
					LA-ICP-MS	LIBS	SIMS
Unheated							
SY001–002	2	Yellow	Sri Lanka	0.23–0.76	bdl	bdl	na
SP001–002	2	Padparadscha	Sri Lanka	0.63–0.85	bdl	na	na
EO001–002	2	Orange	East Africa	0.30–1.32	bdl	na	na
MB001–002	2	Blue	Madagascar	1.23–2.12	bdl	na	na
SCL001–003	3	Colorless	Sri Lanka	0.57–0.68	bdl	na	na
VCS001–010	10	Colorless	Verneuil synthetic	0.85–1.03	bdl	na	na
Traditionally heated							
SY003–004	2	Yellow	Sri Lanka	1.56–3.87	bdl	na	na
EO003–004	2	Orange	East Africa	0.47–2.31	bdl	na	na
MP001–004	4	Pink	Madagascar	0.42–4.01	bdl	na	na
TPL001–002	2	Purple	Tanzania	0.59–2.50	bdl	na	na
MB003–005	3	Blue	Madagascar	1.56–3.52	bdl	na	na
ECC001–002	2	Color change (dark purple)	East Africa	0.40–4.01	bdl	na	na
SCL004–005	2	Colorless	Sri Lanka	0.50–0.71	bdl	na	na
TR001–002	2	Ruby (dark red)	Thailand	0.83–2.59	bdl	na	na
Be-diffusion treated[b]							
SY-H1–H8	8	Yellow	Sri Lanka	0.63–2.96	1.8–8.1	Detected (very low)[c]	na
MPd-H1–H12	12	Pinkish orange	Madagascar	0.34–4.36	bdl–8.4[d]	Detected[e]	bdl–9.54[d]
EO001–003	3	Saturated orange	East Africa	0.23–1.21	3.6–4.1	na	na
EO004–007	4	Orange	East Africa	0.34–3.90	1.9–2.2	na	na
MP-H1–H4	4	Pink	Madagascar	0.63–3.59	1.9–3.3	Detected[f]	na
TPL-H1–H10	10	Purple	Unknown	0.32–3.81	2.6–7.8	na	na
MB-H1–H10	10	Blue	Madagascar	0.89–3.68	1.4–6.3	na	na
MB-H11–H16	6	Blue	Australia	3.82–4.77	3.4–15	na	na
MB-H17–H20	4	Blue	China	2.65–5.26	2.9–6.7	na	na
ECC001	1	Dark green-purple	East Africa	0.32	2.6	na	na
ECC002	1	Dark purple	East Africa	3.93	1.7	na	na
SCL001–002	2	Light yellow	Sri Lanka	0.48–0.56	1.4–5.4	na	na
SCL003–004	2	Light yellow	Sri Lanka	0.40–0.62	bdl–2.3	na	na
TR001–002	2	Ruby (bright red)	Thailand	0.70–2.50	6.3–16	na	na
TR003–004	2	Ruby (bright red)	Thailand	1.13–2.52	0.43–2.43	na	na
VCS001–004	4	Colorless	Verneuil synthetic	0.72–0.81	1.1–5.0	na	na
VCS005–008	4	Colorless	Verneuil synthetic	0.77–0.94	bdl–1.6	na	na
FPS001	1	Whitish pink	Flux synthetic	0.54	4.7	na	na
FPS002	1	Pink	Flux synthetic	0.66	0.3	na	na

[a] *All analyses were performed on the girdle of faceted stones (the Be-diffused samples were repolished after treatment). For LA-ICP-MS: External standard = NIST SRM 612, internal standard = 99.00% Al_2O_3. For SIMS: Accuracy of Be is ±10%, detection limit is 0.01 ppm Be, external standard = Be-implanted synthetic corundum. The following samples were analyzed by LA-ICP-MS before and after Be-diffusion treatment: EO001–004, ECC001–002, SCL001–004, TR001–002, and VCS001–008. These data include one point analysis of the re-polished girdle and eight point analyses of the cross-sections of samples SCL001, SCL003, VCS001, and VCS005. Abbreviations: bdl=below detection limit, na=not analyzed.*

[b] *Samples shown in blue were Be-diffused in Bangkok for 22 hours at 1800°C, whereas the samples shown in green were Be-diffused in Chanthaburi for approximately 10 hours. The exact conditions are not known for the Be-diffusion treatment of samples SY-H1–H8, MPd-H1–H12, MP-H1–H4, TPL-H1–H10, MB-H1–H10, MB-H11–H16, and MB-H17–H20.*

[c] *Sample SY-H1 only.*

[d] *Sample MPd-H1 only: six point analyses of the sample's cross-section using both LA-ICP-MS and SIMS.*

[e] *Sample MPd-H10 only.*

[f] *Sample MP-H4 only.*

converted to weight percent (wt.%) oxides from their simple elemental concentrations (ppm).

To compare the accuracy of our LA-ICP-MS analyses to those obtained with SIMS, we analyzed six points on corundum sample MPd-H1 by both techniques. Each point analyzed by LA-ICP-MS

TABLE 2. Range of chemical compositions by LA-ICP-MS of emeralds from eight localities.[a]

Property	Kaduna, Nigeria	Kafubu, Zambia	Sandawana, Zimbabwe	Itabira-Nova Era, Brazil	Santa Terezinha, Brazil	Swat, Pakistan	Panjshir, Afghanistan	Cordillera Oriental, Columbia
Sample no.	ENNIO1–10	ENZA01–10, EZ100–110	ENZI01–10	EBI001–014	EBS001–015	ENPAI01–10	EAF001–012	ENCO01–10, 1EC001–010
No. of samples	10	20	10	14	15	10	12	20
Color	Bluish green to light green	Bluish green to green	Pale green to green	Green to deep green	Green to deep green	Green to deep green	Pale green to green	Pale green to green to deep green
Weight	0.59–1.07	0.19–3.29	0.13–0.77	0.32–2.25	0.55–3.01	0.15–0.83	0.20–1.77	0.45–3.67
Type	Rough and parallel polished plates	Mixed cuts and parallel polished plates	Parallel polished plates and cabochons	Mixed cuts	Mixed cuts	Parallel polished plates and cabochons	Mixed cuts	Parallel polished plates, cabochons, mixed cuts
Minor elements (wt.% oxides)								
Na_2O	0.22–0.64	0.93–1.87	1.97–2.30	1.33–2.18	1.61–2.43	1.11–2.01	0.79–1.55	0.33–0.82
MgO	0.04–0.09	1.41–2.36	0.88–3.13	1.78–2.54	2.17–2.82	1.86–2.65	0.75–1.82	0.05–1.33
FeO^{tot}	0.48–0.96	1.23–2.17	0.34–1.13	1.13–1.42	1.42–2.34	0.30–1.29	0.28–0.76	bdl–0.23
K_2O	0.006–0.07	0.03–0.42	0.01–0.12	0.02–0.05	0.04–0.91	0.01–0.05	bdl–0.05	bdl–0.02
CaO	0.03–0.07	bdl–0.06	0.05–0.28	bdl–0.02	0.10–0.26	0.01–0.06	bdl–0.02	bdl–0.001
Sc_2O_3	0.003–0.03	0.006–0.04	0.01–0.09	bdl–0.01	bdl–0.02	0.01–0.49	0.001–0.27	bdl–0.001
V_2O_3	0.01–0.06	0.01–0.04	0.02–0.10	0.03–0.07	0.001–0.10	bdl–0.06	0.16–0.50	0.11–1.21
Cr_2O_3	0.01–0.55	0.10–0.80	0.41–1.41	0.09–1.10	0.25–2.66	0.10–0.84	0.30–0.41	0.01–0.64
Cs_2O	0.009–0.01	0.07–0.15	0.01–0.30	bdl–0.01	0.36–0.64	bdl–0.02	bdl–0.009	bdl–0.003
Trace elements (ppm)								
Li	54–200	320–1,260	161–1,370	90.5–305	220–954	163–500	98–229	10–92
B	bdl–2.3	bdl–10	bdl–2.0	bdl	bdl	bdl–2.1	bdl	bdl
Ti	5.0–63	8.2–30	3.1–61	5.2–15	2.6–55	3.5–53	bdl–30	bdl–51
Mn	4.0–43	9.3–156	5.0–180	10–39	9.3–37	bdl–29	9.3–42	bdl–4.4
Co	bdl–1.3	1.9–10	1.2–7.5	bdl–4.9	bdl–3.0	bdl–3.2	bdl–5.4	bdl
Ni	bdl–6.1	6.1–44	3.2–62	17–26	21–105	2.3–26	bdl–27	bdl–5.2
Cu	bdl	bdl–297	bdl–9.7	bdl–1.4	bdl–7.1	bdl–27	bdl–1.6	bdl–4.9
Zn	14–91	21–970	9.1–254	31–117	6.4–32	bdl–6.9	96–135	bdl–3.9
Ga	10–86	8.1–55	6.0–67	12–33	8.7–25	2.3–14	16–57	3.1–70
Rb	6.0–64	24–319	10–570	37–65	46–110	3.1–38	21–44	bdl–5.7
Sr	bdl	bdl	bdl–14	bdl	5.4–39	bdl	bdl–1.1	bdl–1.4
Sn	bdl–3.4	bdl–4.2	bdl–10	bdl–1.5	bdl–5.8	bdl–3.3	bdl–1.3	bdl–5.1
Ba	bdl–2.0	bdl–20	bdl–5.4	bdl–2.0	bdl–3.5	bdl–6.5	bdl–20	bdl
Pb	bdl–7.2	bdl–110	bdl–8.8	bdl	bdl–7.6	bdl–1.1	bdl–1.4	0.1–180
Bi	bdl	bdl–36	bdl–10	bdl–3.5	bdl–17	bdl–3.5	bdl–4.6	bdl–3.7
Pt	bdl	bdl–8.7	bdl–2.1	bdl–1.0	bdl–4.3	bdl	bdl	bdl–3.1
Au	bdl	bdl–4.5	bdl–1.7	bdl–1.4	bdl–5.1	bdl	bdl	bdl–9.6

[a] Be, Al, and Si were not calculated, and S, P, F, Cl, and H_2O were not measured in this study. The following elements in table 5 were not detected in this study: As, Br, Y, Zr, Ag, Cd, Cd, La, and Ce. Abbreviation: bdl = below detection limit.

consisted of a 30 µm round spot, and 10 seconds of ablation resulted in a crater about 2–3 µm deep. The SIMS data were obtained at the Foundation of Promotion for Materials Science and Technology of Japan in Tokyo using a Cameca IMS-6f instrument. A beam current of 150 nA and accelerating voltage of 14.5 kV was used. The beam was composed of O^{2+}. The surface of the sample was analyzed in a minute square pattern measuring 30 × 30 µm, to a depth of about 150 nm. The sputtering rate was approximately 0.15 nm/s, under a vacuum of 3×10^{-7} Pascal (or about one-quadrillionth of atmospheric pressure at sea level). For both the SIMS and LA-ICP-MS analyses of sample MPd-H1, beryllium concentrations were determined using a Be-ion-implanted external standard of pure synthetic corundum. (The Be-ion-implanted synthetic corundum was not used for the other LA-ICP-MS analyses of corundum in this article because its Be content was homogeneous to only a shallow level [i.e., within several nanometers to several hundred nanometers of the surface].)

LIBS data were collected with an Ocean Optics 2000+ instrument at the GAAJ Research Laboratory

in Tokyo. This instrument was developed recently for gemological applications by the SSEF Swiss Gemmological Laboratory in cooperation with the manufacturer (Krzemnicki et al., 2004; Hänni et al., 2004). To investigate the detection limit of Be, we selected seven samples of Be diffusion–treated corundum (SY001–002, SY003–004, SY-H1, MPd-H10, and MP-H4) for comparison of the LIBS results with those from LA-ICP-MS. The LIBS spectra were obtained with Ar gas in the sample chamber and a 1064 nm Nd:YAG laser (from Big Sky Quantel). The girdle of each sample was subjected to 20 single laser shots with a laser energy of 30 mJ, resulting in a laser hole measuring 100 µm in diameter. Emission spectra of detectable elements were recorded in the range of 200–980 nm.

TABLE 3. LA-ICP-MS operating conditions.

ICP-MS parameters	
Radio frequency (RF) power	1500 watts
Carrier gas flow rate	Ar ~1.20–1.23 L/minute, He 0.50 L/minute
Distance from the ICP torch to the sampler	7 mm
Sampler and skimmer	Ni; 1 and 0.4 mm diameters
Mass number (m/z)	2–260
Integration time	0.1 seconds per point (corundum) or 0.01 seconds per point (emerald)
Laser ablation parameters	
Wavelength	213 nm Nd:YAG laser
Pulse duration	5–10 nanoseconds
Pulse frequency	10 Hz
Output power	2.5 mJ
Laser line size	16 µm in width, logo size 8 × 230 µm, 4–7 µm in depth
Laser point size	30 µm diameter, 2–3 µm deep
Pre-ablation time	5 seconds
Ablation time	25 seconds
ICP-MS data acquisition time	40 seconds
Isotope signals selected	
Be-diffused corundum	
Isotopes analyzed	$^{9}Be^{+}$
Signals monitored	$^{27}Al^{+}$, $^{47}Ti^{+}$, $^{53}Cr^{+}$, $^{56}Fe^{+}$, $^{57}Fe^{+}$, $^{69}Ga^{+}$
Emeralds	
Isotopes analyzed	$^{7}Li^{+}$, $^{11}B^{+}$, $^{23}Na^{+}$, $^{24}Mg^{+}$, $^{39}K^{+}$, $^{43}Ca^{+}$, $^{44}Ca^{+}$, $^{45}Sc^{+}$, $^{47}Ti^{+}$, $^{51}V^{+}$, $^{53}Cr^{+}$, $^{55}Mn^{+}$, $^{56}Fe^{+}$, $^{57}Fe^{+}$, $^{59}Co^{+}$, $^{60}Ni^{+}$, $^{63}Cu^{+}$, $^{66}Zn^{+}$, $^{69}Ga^{+}$, $^{85}Rb^{+}$, $^{88}Sr^{+}$, $^{118}Sn^{+}$, $^{133}Cs^{+}$, $^{137}Ba^{+}$, $^{195}Pt^{+}$, $^{197}Au^{+}$, $^{208}Pb^{+}$, $^{+209}Bi^{+}$
Signals monitored	$^{9}Be^{+}$, $^{27}Al^{+}$, $^{28}Si^{+}$, $^{29}Si^{+}$

Figure 4. During the laser ablation process, our research showed that inscribing the GAAJ logo on the girdle of a gemstone provided sufficient material for analysis of one area; this inscription also proves that a sample has been analyzed by LA-ICP-MS. The tiny mark measures 80 × 230 µm and penetrates the stone to a depth of ~5–10 µm. Photomicrograph by A. Abduriyim; magnified 80×.

PRACTICAL APPLICATIONS

Be-diffused Corundum. Mass spectra for typical LA-ICP-MS analyses of corundum are shown in figure 5, as obtained by ablating the GAAJ logo using the conditions summarized in table 3. A detectable beryllium signal is shown in figure 5 for a Be-diffused sapphire, whereas the samples that did not undergo Be diffusion treatment have only a background signal for Be. As shown in table 1, Be was below the detection limit (i.e., <0.1 ppm)[1] in all the unheated and traditionally heated corundum samples of various colors (40 pieces in total). However, Be (on the order of several parts per million) was detected in all corundum samples, natural and synthetic, that had been treated by Be diffusion (81 pieces; see, e.g., figure 6). In the 20 samples analyzed before and after Be diffusion, no Be was detected before treatment but significant amounts were measured in all samples after treatment, regardless of whether any color alteration occurred. No significant color alteration was seen in any of the samples

[1] In this article, we use ppm to indicate the concentration of trace elements. The concentration also can be written as ppmw (parts per million by weight), which is a fractional weight. The concentration of ions, as ion/cm^3, is typically expressed as ppma (parts per million atomic). The mutual relation between these units is approximated by the following expression:

$$ppma = \left[\frac{(molecular\ weight\ of\ Al_2O_3)}{5 \times (atomic\ weight\ of\ element)}\right] \times ppmw$$

treated for approximately 10 hours (figure 7). With the 22-hour heating process, the synthetic sapphires remained colorless, whereas the natural sapphires became yellow.

The concentration of Be was higher in the stones that were heated for 22 hours at 1800°C than in those that were treated for approximately 10 hours. Figure 8 illustrates the Be concentrations measured across some representative samples. The stones that were treated for 22 hours contained 4.2–4.4 ppm Be at the rim and 1.1–1.4 ppm at the center, and the repolished girdles had 5.0 and 5.4 ppm Be. In contrast, the samples treated for the shorter time period contained only 1.0–1.3 ppm Be at the rim, with no Be detected in the core, and the repolished girdles contained 1.6 and 2.3 ppm Be.

TABLE 4. LA-ICP-MS detection limits for this study.[a]

Mass	Element	Average counts (10 empty runs)	Detection limits 3σ (ppm)
7	Li	1,067	1.9
9	Be	11	0.1
11	B	152	1.6
23[b]	Na	4,321	17
24	Mg	57	0.4
27	Al	137	0.8
28[b]	Si	38,187	540
29[b]	Si	1,532	410
39	K	761	3.4
43[b]	Ca	96	230
44[b]	Ca	1,423	240
45	Sc	85	0.3
47	Ti	11	0.6
51	V	44	0.1
53	Cr	353	14
55	Mn	122	0.4
56[b]	Fe	2,630	12
57[b]	Fe	72	7.1
60	Ni	28	0.5
63	Cu	39	0.3
66	Zn	78	2.0
69	Ga	30	0.1
85	Rb	15	0.1
88	Sr	4	0.01
118	Sn	60	0.5
133	Cs	23	0.1
137	Ba	3	0.1
195	Pt	19	0.1
197	Au	24	0.1
208	Pb	34	0.1
209	Bi	28	0.1

[a] *The average intensity of 10 empty runs was used to determine the detection limit of each element. 3σ = 3 standard deviations.*

[b] *Mass interferences are created by polyatomic ions formed from the combination of species derived from the plasma gas, sample matrix, etc. For example, $^{12}C^{16}O$ overlaps ^{28}Si, $^{40}Ar^{16}O$ overlaps ^{56}Fe, $^{28}Si^{16}O$ overlaps ^{44}Ca, $^{40}Ca^{16}O$ overlaps ^{56}Fe, and ^{23}Na contamination from NIST SRM 612 overlaps ^{23}Na from the sample. High background counts for Na, Si, Ca, and Fe were caused by mass interference.*

Comparative analyses of the cross-section of Be-diffused pinkish orange sapphire MPd-H1 using LA-ICP-MS and SIMS techniques are graphed in figure 9. The stone showed no concentrations of Be in the center and high concentrations in the rim. The pattern of Be concentration is very similar for both techniques, with slightly lower values obtained with LA-ICP-MS. For example, at the edge of the sample the Be concentration was measured at about 9.5 ppm with SIMS and 8.0 ppm with LA-ICP-MS. The laser ablation pit was deeper than that vaporized by the SIMS beam, so it is clear that as the depth of ablation increases, the ratio of Be to intrinsic elements decreases. While the exact ablation depth cannot be controlled when using LA-ICP-MS, SIMS has a high spatial resolution that therefore can be used for depth profiling across a sample.

Results from the LIBS study are shown in figure 10, which presents the emission spectra of three corundum samples that underwent Be-diffusion and four that did not. There was no Be emission at 313.068 nm in the spectra of the unheated yellow sapphires (SY001-002). In the spectra of the traditionally heated yellow sapphires (SY003-004), an emission peak at 313.16 nm was detected which overlapped parts of Be spectra, with an intensity of just two counts. However, LA-ICP-MS found no measurable Be in that sample, but did show traces of vanadium. Emission related to V occurs at 313.16 nm in the LIBS spectra, which is close to the wavelength of Be emission.

A small Be emission peak (~2–3 counts) was detected in one Be-diffused yellow sapphire (SY-H1) in which 1.8 ppm Be was measured by LA-ICP-MS. Much higher Be concentrations were measured by LA-ICP-MS in a pink sapphire (MP-H4, 3.3 ppm) and in a pinkish orange sapphire (MPd-H10, 8.4 ppm), and these samples had Be peaks in the LIBS spectra of ~5–6 counts and ~10–11 counts, respectively. For very low intensities of Be emission at 313.068 nm, such as 2–3 counts, it is difficult to determine with LIBS whether or not a sample has been Be-diffusion treated; such stones should be tested on another area of the sample, or by another method such as LA-ICP-MS.

Implications. With the increased use of LA-ICP-MS in gem laboratories and the importance of detecting low ppm levels of Be in corundum, the need for standardization between gemological labs has grown.

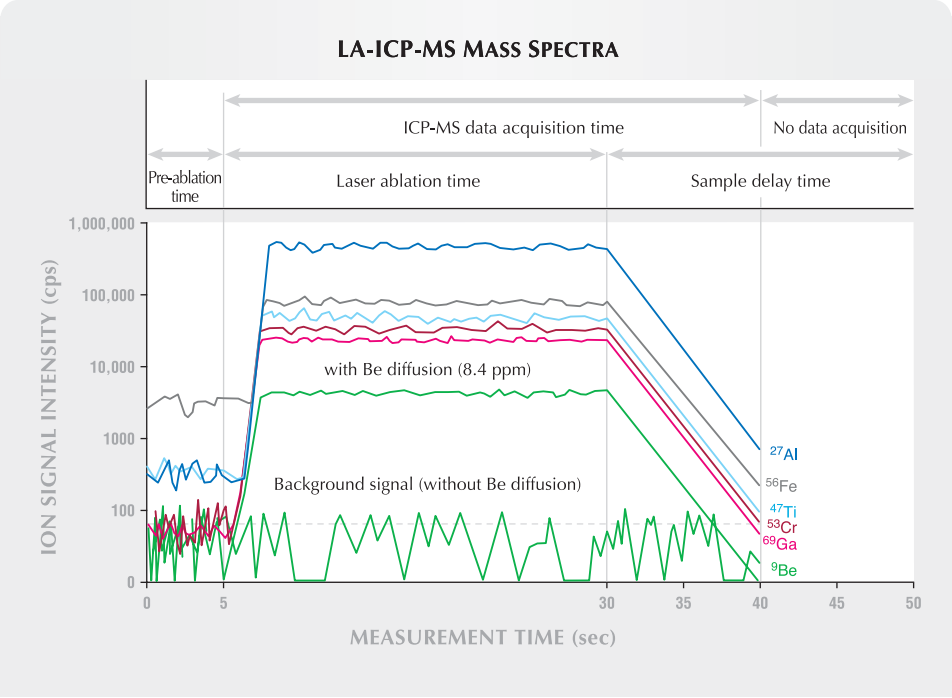

Figure 5. Mass spectra for Be in corundum were generated by laser ablating the GAAJ logo for a 25-second period. The pre-ablation time was 5 seconds, and 35 seconds were used for ICP-MS data acquisition. A detectable Be signal is shown for a Be-diffused sapphire, whereas samples that were either not heated or had been heated by traditional methods do not show a Be signal above the background level. Signals for Al and the common trace elements in corundum (Ti, Cr, Fe, and Ga) were monitored, as shown here, but the concentrations of these elements were not calculated for this study.

Clearly, a high level of confidence is needed in such analyses and a similar level of consistency is desired when comparing results between laboratories. While the results presented here are valid for the conditions of this study, the authors continue to work with other laboratories (particularly members of the Laboratory Manual Harmonization Committee) on an internationally agreed set of analytical parameters and standards.

Under normal geologic conditions, it is difficult for Be atoms to enter the corundum lattice. However, natural corundum contains various types of inclusions (crystals, clouds, silk, etc.) that may host small amounts of Be. Further investigations into the chemical composition of inclusions in natural corundum are under way.

At present and notwithstanding ongoing research, GAAJ believes that when the concentration of Be is

Figure 6. These Be-diffused sapphires and rubies (0.45–3.98 ct) are typical of the material that was analyzed by LA-ICP-MS for this study. Photo by Masaaki Kobayashi.

Figure 7. Verneuil colorless synthetic sapphires (top left, samples VCS001–008, 0.86–1.01 ct) and four of the five natural colorless sapphires (top right, samples SCL001–004, 0.50–0.68 ct) were treated by Be diffusion, half for approximately 10 hours (center row) and half for 22 hours (bottom row) at 1800°C in an oxidizing environment. The synthetic sapphires remained colorless even after 22 hours of Be diffusion (bottom left), whereas yellow color was produced in the natural sapphires SCL001–002 after 22 hours of Be diffusion (bottom right). Photos by Masaaki Kobayashi.

lower than the LA-ICP-MS detection limit of about 0.1 ppm (or 0.2 ppma), and internal features indicate that the corundum has been heated (see, e.g., Emmett et al., 2003; Wang et al., 2006), the stone should be identified as having undergone traditional heat treatment (i.e., without beryllium diffusion). The laboratory report may state "indications of heating" only. However, care should be taken to ensure that proper parts of the stone are analyzed (e.g., at least three areas that are free from potentially interfering inclusions).

GAAJ's present policy also states that when a heat-treated stone contains more than 1 ppm (or 2 ppma) of Be by LA-ICP-MS (using the external NIST glass standards), in areas that are free of inclusions, this stone should be identified as Be diffused. The laboratory report in this case should state that the stone shows "indications of heating, (shallow) color induced by (lattice) diffusion of a chemical element(s) from an external source" (Laboratory Manual Harmonization Committee Information Sheet #2, February 2004; available at www.agta-gtc.org/information_sheets.htm).

Be diffusion–treated corundum commonly has a Be concentration ranging from a few to several hundred ppm. These values are sufficient to indicate Be-diffusion treatment, but the fact that some Be-diffused sapphires contain very low Be concentrations creates challenges for the laboratory gemologist. For example, if a very small amount of Be (e.g., less than 1 ppm) is measured in several analyses of a stone from areas that are *free of inclusions*, this may, until ongoing research is completed, be regarded as falling within an area of uncertainty and this fact should be reflected in the identification report.

Based on our experience using LIBS for routine corundum testing at GAAJ since May 2005, we feel that this technique can detect a minimum of ~1–2 ppm (or 2–5 ppma) Be in corundum. Therefore, LIBS would not be expected to reliably detect the very low concentration of Be mentioned above.

Geographic Origin Determination of Emerald. Emerald crystallizes in complex geologic environments, and the crystals may reflect abrupt changes in

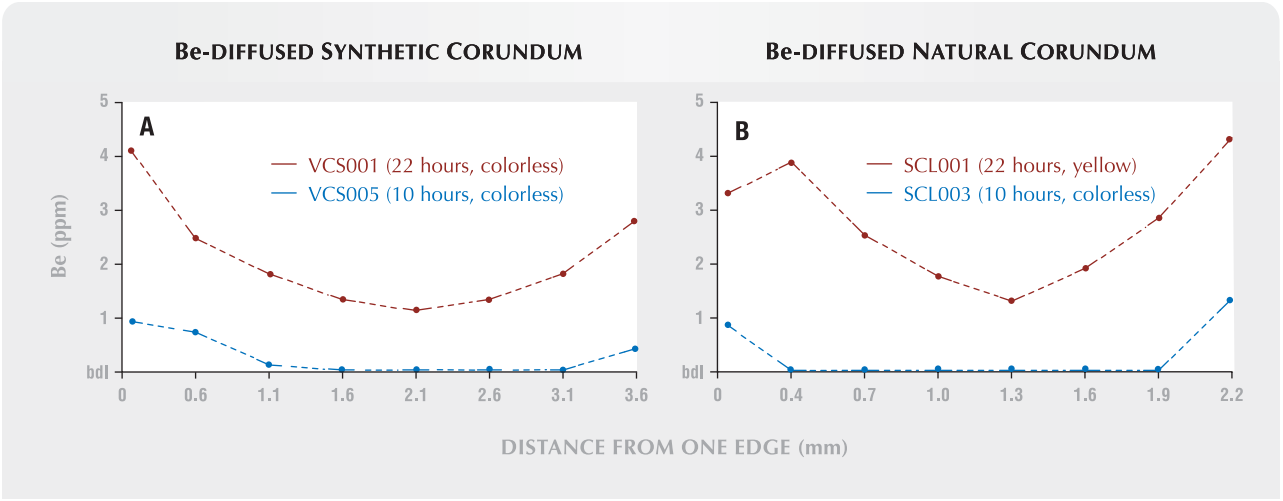

Figure 8. These graphs show the distribution of Be concentrations across cut cross-sections of synthetic sapphires VCS001 and VCS005 (left; 3.5 mm traverse) and natural sapphires SCL001 and SCL003 (right; 2.1 mm traverse) that underwent Be diffusion for different amounts of time. Considerably more Be was recorded in the samples that were diffused longer; both pairs showed Be enrichments near their edges. (The relative error in the analyses is estimated to be ±0.5 ppm Be.) No color modifications were seen in the synthetic sapphires, whereas the natural sapphires changed from colorless to yellow, but only after the longer period of Be diffusion (see figure 7).

the geologic environment and/or mechanical stress. In contrast, other gem beryls, such as aquamarine, develop in relatively stable environments (e.g., within cavities in granitic pegmatites). Emeralds have been mined from the five major continents, with famous localities in South America (Colombia and Brazil), Asia (Russia, Pakistan, and Afghanistan), and Africa (Zambia and Zimbabwe), as well as Madagascar. The geologic characteristics of emerald deposits have been classified into two groups (Schwarz and Giuliani, 2000; Schwarz, 2004) as follows:

Group 1—Crystallization associated with pegmatites
- *Category A:* Pegmatite without schist-related

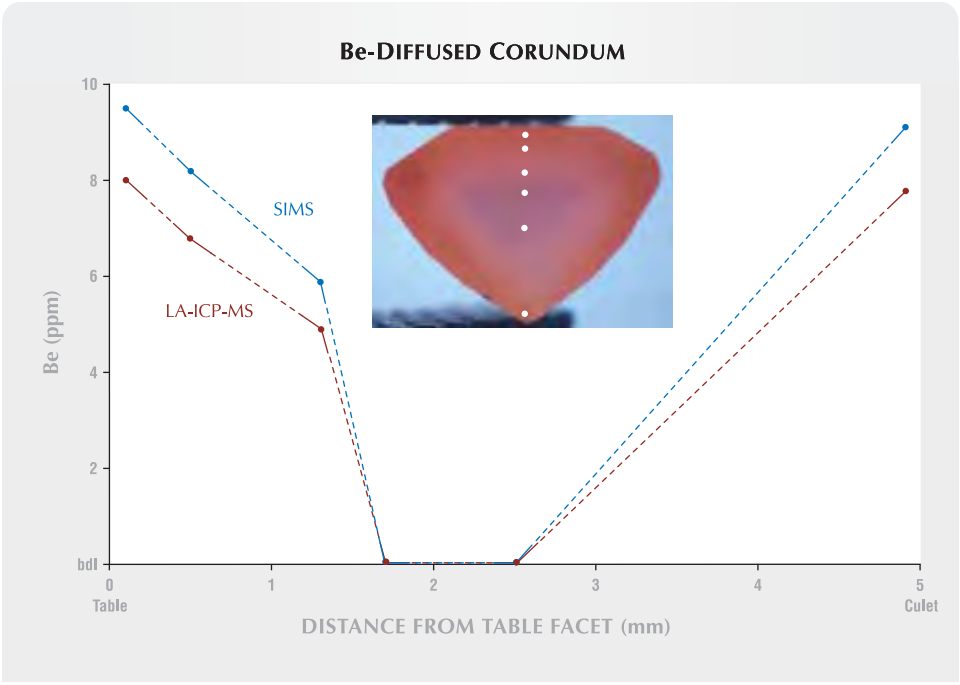

Figure 9. The cut cross-section of a Be-diffused pinkish orange sapphire (sample MPd-H1) was analyzed for Be with both LA-ICP-MS and SIMS, using an external standard of Be-implanted synthetic corundum. The (natural) pink core of the sapphire is surrounded by orange and orangy pink outer zones that resulted from Be diffusion. Slightly higher Be concentrations were consistently measured in the SIMS analyses, except in the pink core, which did not contain any detectable Be by either technique.

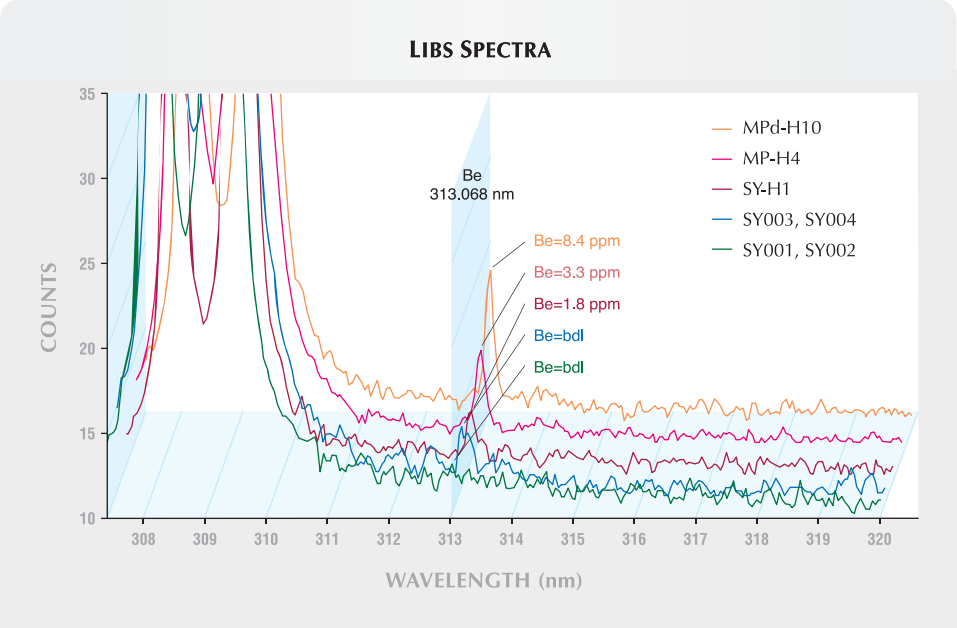

Figure 10. LIBS spectra are shown in the range of 307–320 nm for non-heated sapphires (SY001 and SY002), traditional heat-treated sapphires (SY003 and SY004), and Be diffusion-treated sapphires (SY-H1, MP-H4, and MPd-H10). The Be emission peak is located at 313.068 nm. The large peaks around 308 and 309 nm are due to Al. Be was only detected in the samples that underwent Be diffusion treatment.

emerald (Kaduna, Nigeria)
- *Category B:* Pegmatite and greisen with schist-related emerald (Kafubu, Zambia; Sandawana, Zimbabwe; and Itabira–Nova Era, Brazil)

Group 2—Crystallization without the involvement of pegmatites
- *Category C:* Metamorphic phlogopite schist–related emerald (Santa Terezinha, Brazil)
- *Category D:* Talc-carbonate schist–related emerald (Swat, Pakistan)
- *Category E:* Muscovite schist–related emerald (Panjshir, Afghanistan)
- *Category F:* Black shale with vein- and breccia-related emerald (Cordillera Oriental, Colombia)

Representative emeralds from each of these geologic deposit types were selected for this study (see table 2 and figure 11). LA-ICP-MS analyses of 111 gem-quality emeralds from the eight localities are summarized in table 2. The minor elements Na, Mg, and Fe and the trace elements K, Ca, Sc, V, Cr, and Cs were converted to oxide weight percent values for comparison with data reported on emeralds from the literature: Kaduna (Lind et al., 1986; Schwarz, 1996), Kafubu (Milisenda et al., 1999; Zwaan et al., 2005),

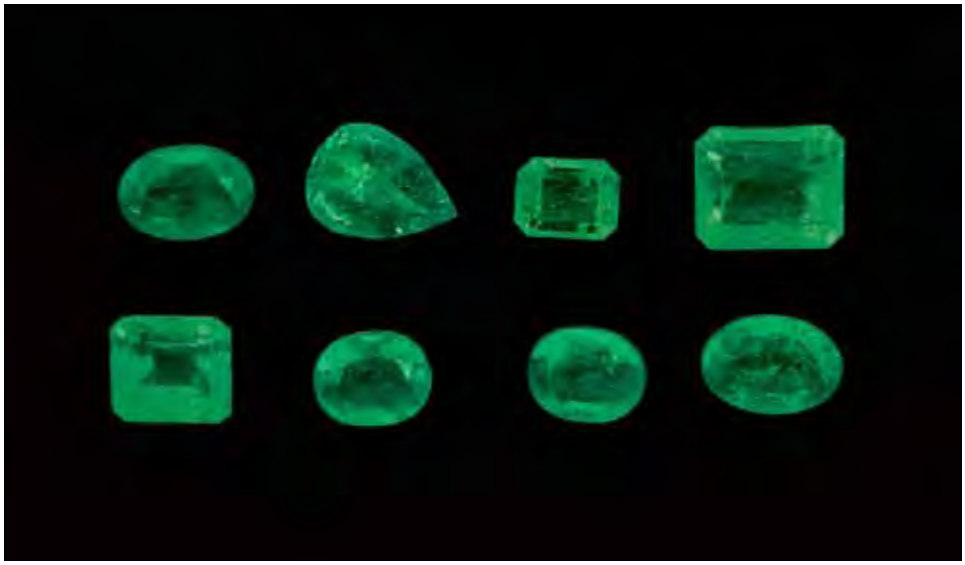

Figure 11. These emeralds are from the eight deposits that were analyzed by LA-ICP-MS for this study. From left to right, top row: Santa Terezinha, Brazil (0.72 ct); Swat, Pakistan (0.83 ct); Panjshir, Afghanistan (0.48 ct); and Cordillera Oriental, Colombia (1.73 ct). Bottom row: Kaduna, Nigeria (1.07 ct); Kafubu, Zambia (0.57 ct); Sandawana, Zimbabwe (0.68 ct); and Itabira–Nova Era, Brazil (0.78 ct). Photo by Kohei Yamashita.

Sandawana (Zwaan et al., 1997), Itabira–Nova Era (Schrader, 1987; Schwarz, 1990b; Kanis, 2001; Zwaan, 2001), Santa Terezinha (Hänni and Kerez, 1983; Schwarz, 1990a; Moroz et al., 1998; Pulz et al., 1998), Swat (Henn, 1988; Hammarstrom, 1989), Panjshir (Hammarstrom, 1989; Moroz et al., 1998) and Cordillera Oriental (Moroz et al., 1998). In addition, the trace elements Li, Ti, Zn, Ga, and Rb were all present in detectable quantities. However, B, Mn, Co, Ni, Cu, Sr, Sn, Ba, Pb, Bi, Pt, and Au were near or below the detection limits of our instrument.

Average data for each of the 111 emeralds from the eight localities are plotted in two different chemical fingerprint diagrams (separate plots for minor and trace elements). The oxide weight percent ratios of the minor elements Cs_2O+K_2O versus FeO+MgO are plotted in figure 12. Based on Cs_2O+K_2O content, the Santa Terezinha, Kafubu, and Sandawana emeralds could be separated from the Kaduna, Panjshir, Itabira–Nova Era, and Colombian emeralds. The Cs_2O+K_2O concentrations were particularly high in the Santa Terezinha emeralds. Moreover, the FeO+MgO contents were useful for separating the Kaduna emeralds from the other localities, although there was considerable overlap with Colombian samples. However, a ternary diagram of Zn-Li-Ga (figure 13) was quite effective at separating the Colombian emeralds from the Kaduna specimens, and also the Swat emeralds from the Itabira–Nova Era and Panjshir specimens (which overlap in figure 12). The Swat specimens occupied the Li-dominant field, while emeralds from Sandawana, Kafubu, Itabira–Nova Era, Panjshir, and Santa Terezinha overlapped to various degrees in the Zn-Li region.

The alkali granite–related Kaduna emeralds of Category A were characterized by relatively low Na, Mg, Cs, and K contents. Generally, the elements that are not intrinsic to beryl (i.e., Na, Mg, Fe, V, Cr, Cs, K, and Ca) were lower than 1.5 wt.% oxide, and the concentration of Fe was greater than the sum of the other nonintrinsic elements. The trace elements Li, Ti, Mn, Zn, Ga, and Rb were usually present in concentrations significantly above background.

The emeralds belonging to Category B (Kafubu, Sandawana, and Itabira–Nova Era) are associated with various metamorphic schist rocks containing phlogopite, biotite, talc, carbonate, and actinolite-tremolite (Schwarz et al., 1996). Their contents of Cr, as well as subordinate Na, Mg, and Fe, showed a wide variation. The Mg concentrations (generally between 1.41 and 3.13 wt.% MgO) were higher than those of Na and Fe. Nevertheless, emeralds originating from these three

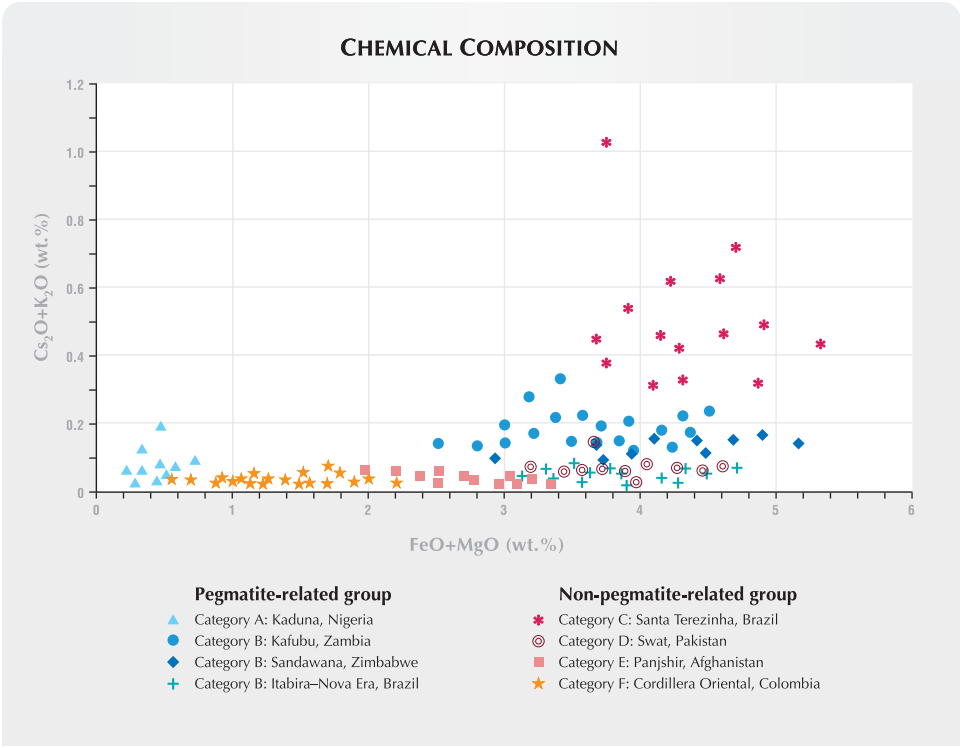

Figure 12. This plot of minor-element concentrations (Cs_2O+K_2O vs. FeO+MgO, in wt.%) of emeralds from the eight localities shows various amounts of overlap. Samples from Santa Terezinha are notable for their high Cs_2O+K_2O contents, whereas those from Kaduna contain the lowest concentrations of all these minor elements.

deposits showed similar ranges of FeO+MgO, and the Zambian samples had the highest sum of Cs_2O+K_2O and relatively enriched trace elements Li, Zn, Rb, and Pb. The Itabira–Nova Era emeralds showed the lowest concentration of Cs_2O+K_2O and overlapped with samples from Category D (Swat). Although the Swat emeralds showed considerable overlap with other categories in figure 13, the trace elements Li, Sc, Mn, Ni, Zn, Ga, and Rb were particularly helpful in distinguishing them.

Category C emeralds from Santa Terezinha are hosted in carbonate-talc-phlogopite schists that had some metasomatic exchange between the Be-bearing fluid and the ultrabasic host rocks (Pulz et. al., 1998). Santa Terezinha emeralds had the highest sum of $Na_2O+MgO+FeO+V_2O_3+Cr_2O_3$ (up to 10 wt.%), and also had the highest Fe, Cr, and Cs concentration measured in this study. In addition, the Santa Terezinha emeralds contained the most Li (up to 950 ppm), with Na>Cs>Li. They also contained the trace elements Ti, Mn, Zn, Ga, and Rb (with Ba and Pb near the detection limits), as well as high levels of Ni, Sr, and Sn.

Emeralds belonging to Category D (Swat, Pakistan), originating from talc-carbonate schist, also had high contents of $Na_2O+MgO+FeO+V_2O_3+Cr_2O_3$, up to 6.85 wt.%. The range of FeO+MgO was distinctly larger than for the Panjshir emeralds of Category E. The different populations of these two deposits are quite evident, especially in the trace elements V, Ga, Rb, and Ba that are enriched in the Afghan emeralds.

Compared to emeralds from the other deposits, the black shale–hosted Colombian emeralds of Category F were rather pure, with only about 4 wt.% of $Na_2O+MgO+FeO+V_2O_3+Cr_2O_3$. Generally Na, Mg, and Fe were low, but the two chromophores V and Cr were anomalously high, up to about 1.85 wt.% for $V_2O_3+Cr_2O_3$. The FeO+MgO content of Colombian emeralds was typically sufficient to distinguish them from neighboring populations of Nigerian and Afghan emeralds.

Implications. Many of the minor and trace elements showed a wider range of concentrations in our samples than were reported previously in the literature (table 5). Mg, K, and V were consistent with the analyses of emeralds reported in most localities, but

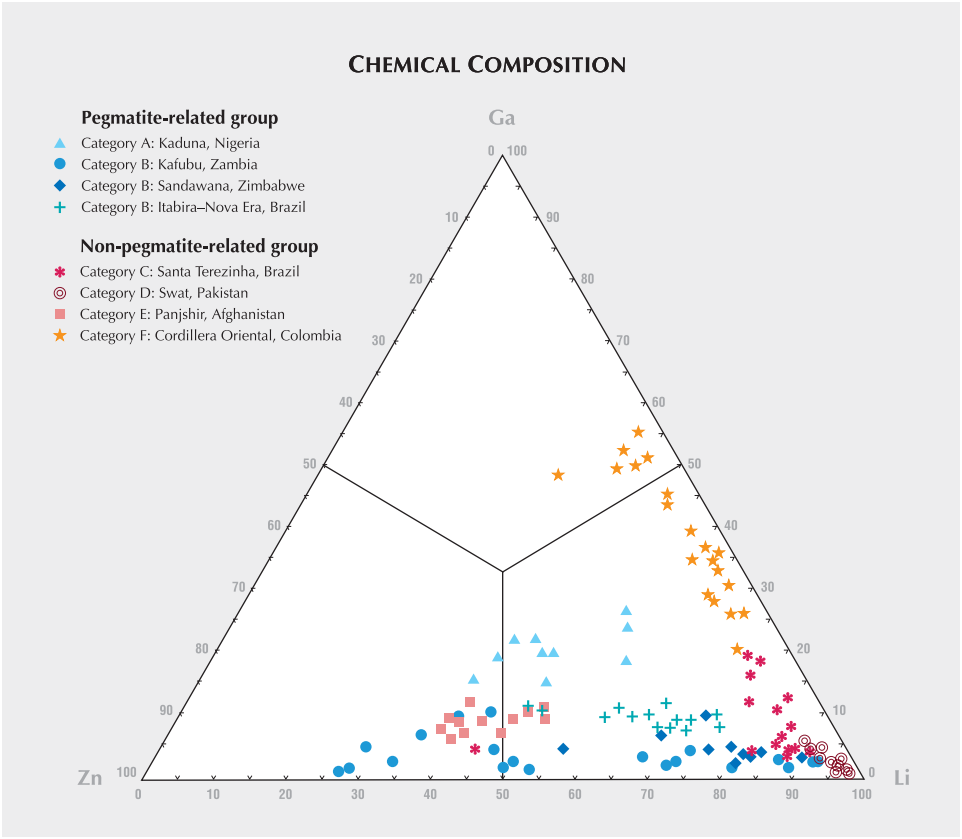

Figure 13. The trace-element concentrations of emeralds from the eight localities are plotted in this Zn-Li-Ga ternary diagram. The Swat and some Santa Terezinha emeralds are Li-dominant, while Colombian stones have intermediate Li-Ga contents. Emeralds from Kafubu, Sandawana, Itabira–Nova Era, and Panjshir are Li-Zn dominant, whereas the Kaduna specimens fall closer to the center of the plot.

our Colombian and Panjshir samples did contain somewhat greater contents of V. In addition, we found more Sc and Cs in emeralds from most of the eight localities; these elements were reported as below or near the detection limits in the literature. The highest amount of Cr found in this study was 2.66 wt.% Cr_2O_3 in emeralds from Santa Terezinha. We measured the highest Fe contents in emeralds from Santa Terezinha and Kafubu, but even greater concentrations of Fe were reported in samples from Swat by Hammarstrom (1989).

Using proton-induced X-ray emission (PIXE), several trace elements that were not measured or detected in our samples (i.e., P, S, Cl, As, Br, Y, Zr, Ag, Cd, La, and Ce) were reported in the literature for emeralds from Kafubu, Sandawana, Santa Terezinha, Swat, and Colombia (again, see table 5). Compared to our LA-ICP-MS data, the PIXE analyses showed relatively high Ti, Mn, Co, Cu, Zn, Ba, Pt, Au, and Bi in emeralds from Kafubu, Sandawana, Santa Terezinha, Swat, and Colombia, but ICP-MS data from Pulz et al. (1998) showed a range similar to that measured in our emeralds from the Santa Terezinha. Using elements such as Li, Zn, Rb, and Pb, it may be possible to differentiate Colombian emeralds (figure 14), arguably the world's most important source, from those of other localities.

Our LA-ICP-MS analyses of emeralds from the eight localities provided no consistent way of clearly distinguishing between pegmatite-related and non-pegmatite-related sources, but the various localities could be separated by a combination of chemical fingerprint diagrams (figures 12 and 13). In figure 12, the Kaduna emeralds correspond to the lowest concentrations of Cs_2O+K_2O and FeO+MgO, although a few data points overlap with the Colombian emeralds. However, there is absolutely no overlap in these localities in figure 13, so Colombian emeralds can easily be separated. Emeralds from Category B (Kafubu, Sandawana, and Itabira–Nova Era) plotted higher in the FeO+MgO field, and can be separated from Santa Terezinha, and Colombian stones on this basis. Swat emeralds completely overlap those from Itabira–Nova Era in figure 12, but figure 13 can be used to make a clear distinction between them. Category B emeralds overlap to some extent in both diagrams, but other trace elements can be used to separate them. Zambian stones showed the greatest sum of Cs_2O+K_2O and high values of Li, Zn, Rb, and Pb. Emeralds from Itabira–Nova Era had the least Cs_2O+K_2O values and low values of Li, Mn, Zn, and Rb. Moderate contents of Cs_2O+K_2O and the highest values of Li, Ti, Mn, and Rb occurred in Sandawana emeralds. Notably, Santa Terezinha, which is one of the major sources of emerald in the market, had the highest concentrations of Fe, Cr, and Cs, with relatively high contents of Li, Ni, and Sr, enabling them be separated from Colombian emeralds. Therefore, chemical data obtained by LA-ICP-MS is effective for separating emeralds from each of the eight geographic origins analyzed for this study. However, for added confidence, the chemical data should be supported by optical properties and internal characteristics that would help substantiate the origin determination. Note that the diagrams provided in this article do not take into account all major emerald sources (e.g., samples from Russia and Madagascar were not included).

COMPARISON OF LA-ICP-MS TO SIMS AND LIBS

The advantages and disadvantages of using LA-ICP-MS, SIMS, and LIBS for analyzing gemstones are listed in table 6. LA-ICP-MS is qualitative to fully quantitative, and can analyze a full range of major, minor, and trace elements, which makes it particularly useful for the geographic origin determination of gem materials. With further research, this technique may prove useful (in certain situations) for determining the geographic origin of diamonds (Watling et al., 1995, Resano et al., 2003, Wang et al., 2003). Note, too, that LA-ICP-MS can be used to analyze solid materials with minimal damage; and because chemical dissolution of the sample is not necessary, there is no solvent-induced spectral interference. Both loose and mounted gem materials can be tested, without need for a conductive coating of carbon or gold and/or other charge balancing techniques, as are required for SIMS and EMPA techniques. For trace-element analysis using a well-characterized standard, a larger number of elements can be accurately quantified with LA-ICP-MS than with SIMS or LIBS. Also, LA-ICP-MS can yield low detection limits, close to that of SIMS (Nenoyer et al., 1991). As with SIMS, the ablation area can be controlled from a minimum crater diameter of several micrometers to a maximum of several hundred micrometers (i.e., greater than the beam diameter that is possible for electron or ion microprobes; Reed, 1989). However, a pit diameter of at least 100 µm is required for LIBS analysis, and there is a risk that the stone may be damaged by the laser.

The disadvantages of LA-ICP-MS analysis include mass interference and element fractiona-

TABLE 5. Chemical compositions of emeralds from the literature, for the eight localities in this study.[a]

Oxides (wt.%)[b]	Kaduna	Kafubu	Sandawana	Itabira-Nova Era	Santa Terezinha	Swat	Panjshir	Cordillera Oriental
	Lind et al., 1986 (4); Schwarz et al., 1996 (16)	Milisenda et al., 1999 (5); Zwaan et al., 2005 (27)	Zwaan et al., 1997 (4)	Schrader, 1987 (1); Schwarz, 1990b (48); Kanis, 2001 (4); Zwaan, 2001 (23)	Hänni et al., 1983 (4); Schwarz, 1990a (14); Moroz et al., 1998 (2)	Henn, 1988 (10); Hammarstrom, 1989 (2)	Hammarstrom, 1989 (3); Moroz et al., 1998 (3)	Moroz et al.,1998 (2)
Na_2O	0.04–0.33	0.74–1.99	2.07–2.41	0.79–1.93	1.46–2.18	1.08–2.11	0.01–1.61	≤0.65
MgO	0.01–0.20	1.26–2.90	2.52–2.75	1.39–2.64	1.27–3.36	2.21–3.10	0.22–1.89	≤0.76
FeO^{tot}	0.11–1.13	0.34–1.31	0.45–0.82	0.41–1.30	0.48–1.82	0.20–2.51	0.21–1.16	≤0.25
K_2O	bdl–0.05	bdl–0.26	0.03–0.06	≤0.08	≤0.16	≤0.02	≤0.09	≤0.03
CaO	bdl–0.01	bdl–0.07	≤0.03	≤0.10	≤0.10	bdl	≤0.07	≤0.23
Sc_2O_3	bdl–0.03	bdl–0.03	bdl	-	-	≤0.19	-	-
V_2O_3	bdl–0.09	bdl–0.06	0.04–0.07	≤0.08	≤0.12	0.04–0.07	0.03–0.29	≤0.21
Cr_2O_3	bdl–0.08	bdl–0.63	0.61–1.33	0.06–1.42	0.06–1.54	0.61–1.33	0.10–0.54	≤0.29
Cs_2O	bdl–0.05	bdl–0.23	0.06–0.10	≤0.01	≤0.20	-	≤0.27	≤0.23

Trace elements (ppm)[c]	Kaduna	Kafubu		Sandawana	Itabira-Nova Era	Santa Terezinha			Swat		Panjshir	Cordillera Oriental
		Yu et al., 2000 (25)	Calligaro et al., 2000 (11)	Calligaro et al., 2000 (22)		Pulz et al., 1998 (5)	Calligaro et al., 2000 (8)	Yu et al., 2000 (5)	Yu et al., 2000 (6)	Calligaro et al., 2000 (4)		Yu et al., 2000 (20)
Li	-	-	580	800	-	24–30	580	-	-	350	-	-
P	-	bdl–433	-	-	-	-	-	bdl	bdl–302	-	-	bdl–224
S	-	bdl–10,707	-	-	-	-	-	175–916	90–422	-	-	83–923
Cl	-	109–1,188	-	-	-	-	-	351–924	227–758	-	-	356–1,864
Ti	-	bdl–89	-	-	-	<118[d]	-	bdl–355	bdl–219	-	-	bdl–115
Mn	-	bdl–156	-	-	-	<154[d]	-	bdl–189	bdl	-	-	bdl–124
Co	-	bdl–262	-	-	-	-	-	bdl	bdl–233	-	-	bdl–110
Ni	-	-	-	-	-	37–97	-	-	-	-	-	-
Cu	-	44–329	-	-	-	2	-	bdl–285	bdl–185	-	-	42–1,070
Zn	-	22–212	-	-	-	2–8	-	50–187	20–93	-	-	bdl–203
Ga	-	19–273	-	-	-	-	-	53–261	17–35	-	-	57–243
As	-	bdl	-	-	-	-	-	bdl–44	bdl	-	-	bdl–32
Br	-	bdl	-	-	-	-	-	bdl–82	bdl–75	-	-	bdl
Rb	-	bdl–120	140	350	-	<168[d]	140	bdl–30	bdl–122	6	-	bdl–61
Sr	-	bdl–29	-	-	-	2–38	-	bdl–91	bdl	-	-	bdl
Y	-	bdl–100	-	-	-	<2	-	bdl	bdl	-	-	bdl–145
Zr	-	bdl–98	-	-	-	<4	-	bdl	bdl	-	-	0
Ag	-	-	-	-	-	<0.4	-	-	-	-	-	-
Cd	-	-	-	-	-	<0.5	-	-	-	-	-	-
Sn	-	-	-	-	-	-	-	-	-	0	-	-
Ba	-	bdl–367	-	-	-	<2	-	bdl–233	282–978	-	-	bdl–1,265
La	-	bdl–474	-	-	-	-	-	175–805	bdl–546	-	-	bdl–1,371
Ce	-	bdl–509	-	-	-	-	-	bdl–669	bdl–443	-	-	bdl–2,335
Pt	-	bdl–392	-	-	-	-	-	bdl–132	bdl–66	-	-	bdl–154
Au	-	bdl–213	-	-	-	-	-	bdl–123	bdl–96	-	-	bdl–260
Pb	-	bdl–252	-	-	-	<5	-	bdl	bdl–86	-	-	bdl
Bi	-	bdl–335	-	-	-	<5	-	bdl–174	bdl–58	-	-	bdl–90

[a] *The number of analyzed samples is shown in parentheses after the corresponding reference. Abbreviation: bdl = below detection limit.*
[b] *Analyzed by EMPA.*
[c] *Analyzed by ICP-MS, except for Pulz et al. (1998), which used particle-induced x-ray emission (PIXE).*
[d] *Calculated as ppm by weight.*

tion. Element isotope determination with the ICP-MS may suffer a strong spectral interference from air entrainment, from the sample's matrix, and from polyatomic ions, resulting in mass spectral overlap and a high background. (With SIMS, the high vacuum required in the sample chamber eliminates the

mass interference from air, but matrix interference is still problematic.) The lack of adequate external standards for calibration for a wide variety of samples of interest makes it difficult to obtain reliable quantitative results for some materials by LA-ICP-MS. Even with the use of a well-characterized standard such as Be ion–implanted synthetic sapphire, LA-ICP-MS is not an effective technique for depth profiling due to fluctuations in the laser power density and the rate of ablation.

Assuming an instrument configuration that is equivalent to that used in this study, the cost of an LA-ICP-MS system is more than US$400,000, whereas a SIMS system exceeds $1,000,000. The newly introduced LIBS equipment is much less expensive, and can range from $50,000 to $90,000, but it is not as effective as LA-ICP-MS and SIMS for providing highly sensitive multi-element quantitative analysis of a small selected area.

CONCLUSIONS

A 213 nm Nd:YAG laser ablation system combined with a quadrupole ICP-MS instrument is a very sensitive and satisfactory method for the analysis of gem materials, as it is capable of ablating the gemstone in a controlled way (e.g., with a laser logo on the girdle of the stone) to obtain a sensitive, stable signal for quantitative chemical analysis. LA-ICP-MS can be used to detect trace levels of Be (i.e., 0.1 ppm) in corundum to detect diffusion treatment, and can also provide data that can be used to create chemical fingerprint diagrams for geographic origin determination.

Figure 14. Emeralds from Colombia have a distinctive chemical composition that is related to their formation in black shale. LA-ICP-MS analysis is therefore useful for separating Colombian emeralds from those of other localities. This 1.77 ct emerald from the Coscuez mine in Colombia was photographed together with the pyrite-bearing black shale host rock. Courtesy of Ronald Ringsrud Co., Saratoga, California; photo © Robert Weldon.

TABLE 6. Comparison of the advantages and disadvantages of LA-ICP-MS, SIMS, and LIBS.

Characteristic	LA-ICP-MS	SIMS	LIBS
Resolution	Highly sensitive	Highly sensitive	Sensitive
Operation	Technical personnel	Technical personnel	Lab staff
Cost of instrument	More than $400,000	More than $1,000,000	More than $50,000
Element detection	Simultaneous multi-element	Simultaneous multi-element	Simultaneous multi-element (based on spectral range of 200–980 nm)
Focusing	CCD auto focus with microscope	CCD auto focus with microscope	Manual
Be detection limit	>0.1ppm (this study)	>0.01ppm (this study)	>2 ppm (Krzemnicki, 2004; Themelis 2004)
Spot size	~5–160 µm	~1–300 µm (beam scan)	>100 µm
Crater depth	More than 1 µm, depending on laser ablation used	Several thousandths to tenths of a µm, depending on beam power	More than several µm, depending on laser ablation used
Laser logo mark	Possible	Impossible	Impossible
Calibration reference	External and/or internal standard	External and/or internal standard	External standard
Sample chamber	No vacuum	High vacuum	No vacuum

ABOUT THE AUTHORS
Dr. Abduriyim (ahmadjan@gaaj-zenhokyo.co.jp) is manager, and Mr. Kitawaki is director, at the research laboratory of the Gemmological Association of All Japan, Tokyo.

ACKNOWLEDGMENTS
The authors thank Dr. Dietmar Schwarz for supplying detailed information on worldwide emerald deposits as well as emerald samples for analysis. Katsuo Mizobuchi and Masahiko Endo at Agilent Technologies in Tokyo provided advice and technical discussion regarding this work. Dr. Ichiro Sunagawa (Tokyo, Japan) and Kenneth Scarratt (GIA Research, Bangkok, Thailand) kindly provided a critical reading and helped revise an early draft of this manuscript.

REFERENCES

Abduriyim A., Kitawaki H. (2006) Determination of the origin of blue sapphire using laser ablation inductively coupled plasma mass spectrometry (LA-ICP-MS). *Journal of Gemmology*, Vol. 30, No. 1–2, pp. 23–36.

Arrowsmith P. (1987) Laser ablation of solids for elemental analysis by inductively coupled plasma mass spectrometry. *Analytical Chemistry*, Vol. 59, No. 10, pp. 1437–1444.

Aston F.W. (1919) A positive-ray spectrograph. *Philosophical Magazine*, Vol. 38, pp. 707–715.

Benninghoven A., Rüdenauer F.G., Werner H.W. (1987) *Secondary Ion Mass Spectrometry: Basic Concepts, Instrumental Aspects, Applications, and Trends*. Wiley, New York, 1227 pp.

Calligaro T., Dran J.C., Poirot J.P., Querré G., Salomon J., Zwaan J.C. (2000) PIXE/PIGE characterization of emeralds using an external micro-beam. *Nuclear Instruments and Methods in Physics Research B*, Vol. 161–163, pp. 769–774.

Dempster A.J. (1918) A new method of positive ray analysis. *Physical Review*, Vol. 11, No. 4, pp. 316–324.

Devos W., Senn-Luder M., Moor C., Salter C. (2000) Laser ablation inductively coupled plasma spectrometry (LA-ICP-MS) for spatially resolved trace analysis of early-Medieval archaeological iron finds. *Fresenius' Journal of Analytical Chemistry*, Vol. 366, No. 8, pp. 873–880.

Dunn P.J. (1977) The use of the electron microprobe in gemology. *Journal of Gemmology*, Vol. 15, No. 5, pp. 248–258.

Emmett J.L., Scarratt K., McClure S.F., Moses T., Douthit T.R., Hughes R., Novak S., Shigley J.E., Wang W., Bordelon O., Kane R.E. (2003) Beryllium diffusion of ruby and sapphire. *Gems & Gemology*, Vol. 39, No. 2, pp. 84–135.

García-Ayuso L.E., Amador-Hernandez J., Fernandez-Romero J.M., Luque de Castro M.D. (2002) Characterization of jewellery products by laser-induced breakdown spectroscopy. *Analytica Chimica Acta*, Vol. 457, No. 2, pp. 247–256.

Gray A.L. (1985) Solid sample introduction by laser ablation for inductively coupled plasma source mass spectrometry. *Analyst*, Vol. 110, No. 5, pp. 551–556.

Günther D., Frischknecht R., Heinrich C.A., Kahlert H.J. (1997) Capabilities of an argon fluoride 193 nm excimer laser for laser ablation inductively coupled plasma mass spectrometry microanalysis of geological materials. *Journal of Analytical Atomic Spectrometry*, Vol. 12, No. 9, pp. 939–944.

Günther D., Heinrich C.A. (1999) Enhanced sensitivity in laser ablation–ICP mass spectrometry using helium-argon mixtures as aerosol carrier. *Journal of Analytical Atomic Spectrometry*, Vol. 14, No. 9, pp. 1363–1368.

Günther D., Kane R.E. (1999a) Laser ablation–inductively coupled plasma–mass spectrometry: A new way of analyzing gemstones. *Gems & Gemology*, Vol. 35, No. 3, pp. 160–161.

Günther D., Kane R.E. (1999b) Laser ablation-inductively coupled plasma–mass spectrometry—A new way of analyzing gemstones. In *Gemmologist's Handbook*, XXXVII International Gemmological Conference, India 1999, Forum of Indian Gemmologists for Scientific Studies, Bombay, p. 25.

Guillong M., Günther D. (2001) Quasi "non-destructive" laser ablation–inductively coupled plasma–mass spectrometry fingerprinting of sapphire. *Spectrochimica Acta B*, Vol. 56, No. 7, pp. 1219–1231.

Hänni H.A., Kezer C.J. (1983) Neues vom Smaragdvorkommem von Santa Terezinha de Goiás, Brasilien. *Gemmologie: Zeitschrift der Deutschen Gemmologischen Gesellschaft*, Vol. 32, No. 1, pp. 50–58.

Hänni H.A., Krzemnicki M.S., Kiefert L., Chalain, J.P. (2004) Ein neues Instrument für die analytische Gemmologie: LIBS. *Gemmologie: Zeitschrift der Deutschen Gemmologischen Gesellschaft*, Vol. 53, No. 2–3, pp. 79–86.

Hammarstrom J.M. (1989) Mineral chemistry of emeralds and some associated minerals from Pakistan and Afghanistan: A electron microprobe study. In A.H. Kazmi and L.W. Snee, Eds., *Emeralds of Pakistan: Geology, Gemology and Genesis*, Van Nostrand Reinhold, New York, pp. 125–150.

Henn U. (1988) Untersuchungen an Smaragden aus dem Swat-Tal, Pakistan. *Zeitschrift der Deutschen Gemmologischen Gesellschaft*, Vol. 37, No. 3/4, pp. 121–127.

Hirata T., Nesbitt R.W. (1995) U-Pb isotope geochronology of zircon: Evaluation of the laser probe-inductively coupled plasma mass spectrometry technique. *Geochimica et Cosmochimica Acta*, Vol. 59, No. 12, pp. 2491–2500.

Horn I., Rudnick R.L., McDonough W.F. (2000) Precise elemental and isotope ratio measurement by simultaneous solution nebulization and laser ablation-ICP-MS: Application to U-Pb geochronology. *Chemical Geology*, Vol. 164, No. 3–4, pp. 281–301.

Jackson S., Pearson N., Griffin W. (2001) In situ isotope ratio determination using laser-ablation (LA)–magnetic sector–ICP-MS. In P. Sylvester, Ed., *Laser-Ablation-ICPMS in the Earth Sciences: Principles and Applications*, Short Course Series, Vol. 29, Mineralogical Association of Canada, St. Johns, Newfoundland, pp. 105–120.

Jarvis K.E., Gray A.L., Houk R.S. (1992) *Handbook of Inductively Coupled Plasma Mass Spectrometry*. Chapman and Hall, New York.

Jeffries T.E., Perkins W.T., Pearce N.J.G. (1995) Comparison of infrared and ultraviolet-laser probe microanalysis inductively–coupled plasma–mass spectrometry in mineral analysis. *Analyst*, Vol. 120, No. 5, pp. 1365–1371.

Jeffries T.E., Jackson, S.E., Longerich H.P. (1998) Application of a frequency quintupled Nd:YAG source (λ = 213 nm) for laser ablation ICP-MS analysis of minerals. *Journal of Analytical Atomic Spectrometry*, Vol. 13, No. 9, pp. 935–940.

Jenner G.A., Foley S.F., Jackson S.E., Green T.H., Fryer B.J., Longerich H.P. (1993) Determination of partition coefficients for trace elements in high pressure-temperature experimental run products by laser ablation microprobe-inductively coupled plasma-mass spectrometry (LAM-ICP-MS). *Geochimica et Cosmochimica Acta*, Vol. 57, No. 23–24, pp. 5099–5103.

Kanicky V., Mermet J.-M. (1999) Use of a single calibration graph for the determination of major elements in geological materials by laser ablation inductively coupled plasma atomic emission spectrometry with added internal standards. *Fresenius' Journal of Analytical Chemistry*, Vol. 363, No. 3, pp. 294–299.

Kanis J. (2001) The Itabira emerald field, MG, Brazil. *28th International Gemmological Conference*, Madrid, Spain, October 8–11. pp. 49–52.

Krzemnicki M.S., Hänni H.A., Walters R.A. (2004) A new method for detecting Be diffusion-treated sapphires: Laser-induced breakdown spectroscopy (LIBS). *Gems & Gemology*, Vol. 40, No. 4, pp. 314–322.

Lind Th., Schmetzer K., Bank H. (1986) Blue and green beryls (aquamarine and emeralds) of gem quality from Nigeria. *Journal of Gemmology*, Vol. 20, No. 1, pp. 40–48.

Loucks R.R., Eggins S.M., Sheglley L.M.G., Kinsley L.P.J., Ware N.G. (1995) Development of the inductively-coupled-plasma mass spectrometry ultraviolet laser trace-element micro-analyzer (ICPMS-ULTEMA). In *Research School of Earth Sciences Annual Report*, Australian National University, Canberra, pp. 138–140.

Milisenda C.C., Malango V., Taupitz K.C. (1999) Edelsteine aus Sambia-Teil 1: Smaragd. *Gemmologie: Zeitschrift der Deutschen Gemmologischen Gesellschaft*, Vol. 48, No. 1, pp. 9–28.

Moroz I.I., Eliezri I.Z. (1998) Emerald chemistry from different deposits: An electron microprobe study. *Australian Gemmologist*, Vol. 20, No. 2, pp. 64–69.

Muhlmeister S., Fritsch F., Shigley J.E., Devouard B., Laurs B.M. (1998) Separating natural and synthetic rubies on the basis of trace-element chemistry. *Gems & Gemology*, Vol. 34, No. 2, pp. 80–101.

Nenoyer E.R., Fredeen K.J., Hager J.W. (1991) Laser solid sampling for inductively coupled plasma mass spectrometry. *Analytical Chemistry*, Vol. 63, No. 8, pp. 445A–475A.

Norman M. (2001) Applications of laser-ablation ICPMS to the trace element geochemistry of basaltic magmas and mantle evolution. In P. Sylvester, Ed., *Laser-Ablation-ICP-MS in the Earth Sciences: Principles and Applications*, Short Course Series, Vol. 29, Mineralogical Association of Canada, St. Johns, Newfoundland, pp. 163–184.

Novak S.W., Magee C.W., Moses T., Wang W. (2004) Using SIMS to diagnose color changes in heated gem sapphires. *Applied Surface Science*, Vol. 231–232, pp. 917–920.

Pearce N.J.G., Perkins W.T., Westgate J.A., Gorton M.P., Jackson S.E., Neal C.R., Chenery S.P. (1997) Application of new and published major and trace elements data for NIST SRM 610 and NIST SRM 612 glass reference materials. *Geostandards Newsletter*, Vol. 21, No. 1, pp. 115–144.

Pollard A.M., Heron H. (1996) *Archaeological Chemistry*. The Royal Society of Chemistry, London.

Pulz G.M., D'el-Rey Silva L.J.H., Barros Neto L.S., Brum T.M.M., Juchem P.L., Santos C.A., Pereira V.P., Silva J.J. (1998) The chemical signature of emeralds from the Campos Verdes-Santa Terezinha mining district, Goias, Brazil. *Journal of Gemmology*, Vol. 26, No. 4, pp. 252–261.

Rankin A.H., Greenwood J., Hargreaves D. (2003) Chemical finger printing of some east African gem rubies by laser ablation ICP-MS. *Journal of Gemmology*, Vol. 28, No. 8, pp. 473–482.

Reed S.J.B. (1989) Ion microprobe analysis: A review of geological applications. *Mineralogical Magazine*, Vol. 53, pp. 3–24.

Resano M., Vanhaecke F., Hutsebaut D., De Corte K., Moens L. (2003) Possibilities of laser ablation-inductively coupled plasma-mass spectrometry for diamond fingerprinting. *Journal of Analytical Atomic Spectrometry*, Vol. 18, No. 10, pp. 1238–1242.

Saminpanya S., Manning D.A.C., Droop G.T.R., Henderson C.M.B. (2003) Trace elements in Thai gem corundums. *Journal of Gemmology*, Vol. 28, No. 7, pp. 399–415.

Scarratt K. (2002) Orange-pink sapphire alert. American Gem Trade Association Gemological Testing Center, www.agta-gtc.org/2002-01-08_orangesapphirealert.htm, January 8.

Schrader H.W. (1987) Natürliche und synthetische Smaragde. Einbeitrag zur Kristallchemie der Berylle. Ph.D. dissertation, Fachbereich Geowissenschaften der Johannes Gutenberg Universität Mainz, Germany.

Schwarz D. (1990a) Die brasilianischen Smaragde und ihre Vorkommen: Santa Terezinha de Goias/GO. *Zeitschrift der Deutschen Gemmologischen Gesellschaft*, Vol. 39, No. 1, pp. 13–44.

Schwarz D. (1990b) Die chemische Eigenschaften der Smaragde I. Brasilien. *Zeitschrift der Deutschen Gemmologischen Gesellschaft*, Vol. 39, No. 4, pp. 233–272.

Schwarz D. (2004) The world of emeralds. *30th Gemmological Conference of All Japan*, Abstracts Volume, Kyoto, Japan, June 12–13.

Schwarz D., Kanis J., Kinnaird J. (1996) Emerald and green beryl from central Nigeria. *Journal of Gemmology*, Vol. 25, No. 2, pp. 117–141.

Schwarz D., Giuliani K. (2000) Emerald deposits: A review. In *Brazil 2000: 31st International Geological Congress*, Abstracts Volume, Aug. 6–17, Rio de Janeiro.

Shida J., Kitawaki H., Abduriyim A. (2002) Investigation of corundum heat-treated by a new technique. *Journal of the Gemmological Society of Japan*, Vol. 24, No. 1–4, pp.13–23.

Stephens W.E. (1946) A pulsed mass spectrometer with time dispersion. *Physical Review*, Vol. 69, No. 11–12, pp. 691.

Stern W.B., Hänni H.A. (1982) Energy-dispersive X-ray spectrometry: A non-destructive tool in gemmology. *Journal of Gemmology*, Vol. 18, No. 4, pp. 285–296.

Stockton C.M., Manson D.V. (1981) Scanning electron microscopy in gemology. *Gems & Gemology*, Vol. 17, No. 2, pp. 72–79.

Themelis T. (2004) LIBS: A spark of inspiration in gemological analytical instrumentation. *Australian Gemmologist*, Vol. 22, pp. 138–145.

Thomson J.J. (1911) Rays of positive electricity. *Philosophical Magazine*, Vol. 6, No. 20, pp. 752–767.

Tye C., Woods G., McCurdy E., Wilbur S. (2004) Semiquantitative analysis—7500 ORS as a powerful & rapid survey tool. *Agilent ICP-MS Journal*, No. 20, pp. 2–3.

Tykot R.H. (2002) Chemical fingerprinting and source tracing of obsidian: The central Mediterranean trade in black gold. *Accounts of Chemical Research*, Vol. 35, pp. 618–627.

Wang W., Hall M., Smith C.P., Shigley J.E. (2003) Applications to diamond testing: A new analytical technique: LA-ICP-MS. *Rapaport Diamond Report*, Vol. 26, No. 33, pp. 177–181.

Wang W., Scarratt K., Emmett J.L., Breeding C.M., Douthit T.R. (2006) The effects of heat treatment on zircon inclusions in Madagascar sapphires. *Gems & Gemology*, Vol. 42, No. 2, pp. 134–150.

Watling R.J., Herbert H.K., Barrow I.S., Thomas A.G. (1995) Analysis of diamond and indicator minerals for diamond exploration by laser ablation–inductively coupled plasma mass spectrometry. *Analyst*, Vol. 120, No. 5, pp. 1357–1364.

Yu N.K., Tang S.M., Tay T.S. (2000) PIXE studies of emeralds. *X-Ray Spectrometry*, Vol. 29, pp. 267–278.

Zwaan J.C., Kanis J., Petsch E.J. (1997) Update on emerald from the Sandawana mines, Zimbabwe. *Gems & Gemology*, Vol. 33, No. 2, pp. 80–100.

Zwaan J.C. (2001) Preliminary study of emeralds from the Piteiras emerald mine, Minas Gerais, Brazil. *XXVIII International Gemmological Conference, Spain 2001, Extended Abstracts*, Oct. 8–11, Madrid, pp. 106–109.

Zwaan J.C., Seifert A.V., Vrana S., Laurs B.M., Anckar B., Simmons W.B., Falster A.U., Lustenhouwer W.J., Muhlmeister S., Koivula J.I., Garcia-Guillerminet H. (2005) Emeralds from the Kafubu area, Zambia. *Gems & Gemology*, Vol. 41, No. 2, pp. 116–148.

Last chance to register for the

GIA®

Gemological Research Conference 2006

August 26–27

Manchester Grand Hyatt Hotel
San Diego, California
Sponsored by Charles & Colvard, Ltd.

Register Now!

THE SCIENCE OF GEMOLOGY is expanding in many exciting directions that encompass not only mineralogy and geology, but also fields such as physics, chemistry, and materials science. At the GIA Gemological Research Conference, a multidisciplinary approach will explore the challenges posed by new synthetic and treated gem materials, as well as the characterization of natural gems from traditional and new sources. Invited lectures, submitted oral presentations, and a poster session will explore a diverse range of contemporary topics in gemology and related sciences.

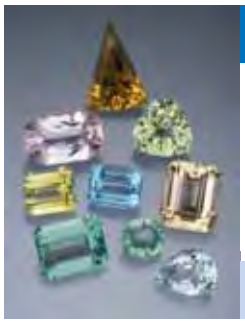

List of Confirmed Presentations Now Available

The titles of confirmed presentations (both oral and poster) for the Gemological Research Conference are now available on the conference website (www.gia.edu/gemsandgemology). The list will be updated as additional presentations are confirmed, and attendees should check periodically for future updates as the conference approaches.

Pala Pegmatite Field Trips—Sold Out

The August 25 and 30 field trips to the Pala pegmatite district have reached full capacity, and there are substantial waiting lists for each trip.

Register Now

The Gemological Research Conference costs only $295 ($395 after August 11), including breakfast and lunch both days, a cocktail reception on August 26, and GIA's 75th Anniversary Gala on August 27. To register for the Gemological Research Conference or the International Gemological Symposium, visit **www.symposium.gia.edu.**

NAVIGATING THE CHALLENGES AHEAD

Keynote Speakers

Geology of Gem Deposits
- **Dr. Jeff Harris,** University of Glasgow, UK
  Diamond occurrence and evolution
- **Dr. David London,** University of Oklahoma, Norman
  Geochemical cycle of certain elements that form gems

Gem Characterization Techniques
- **Dr. George Rossman,** California Institute of Technology, Pasadena *Characterization of nanofeatures in gem materials*
- **Dr. Emmanuel Fritsch,** IMN, University of Nantes, France
  Review and forecast of important techniques in gemology

New Gem Localities
- **Dr. Lawrence Snee,** U.S. Geological Survey, Denver
  Mapping of gem localities in Afghanistan and Pakistan
- **Dr. Federico Pezzotta,** Museo Civico di Storia Naturale, Milan *Update on gem localities in Madagascar*

Gem Synthesis
- **Dr. James Butler,** Naval Research Laboratory, Washington, DC *Growth of CVD synthetic diamond*
- **Dr. Ichiro Sunagawa,** Tokyo *Growth, morphology, and perfection of single crystals: Basic concepts in discriminating natural from synthetic gemstones*

General Gemology
- **Shane McClure,** GIA Laboratory, Carlsbad
  Genetic source type classification of gem corundum
- **Menahem Sevdermish,** Advanced Quality A.C.C. Ltd., Ramat Gan, Israel *Color communication: The analysis of color in gem materials*

Diamond and Corundum Treatments
- **Ken Scarratt,** GIA Research, Bangkok
  Corundum treatments
- **Dr. Mark Newton,** University of Warwick, Coventry, UK
  Diamond treatments

Eight additional speakers for each session will be selected from submitted abstracts.

The GIA Gemological Research Conference will be held in conjunction with the 4th International Gemological Symposium, which will take place August 27–29, 2006. For further information on attending the GIA Gemological Research Conference, contact the organizing committee at:

E-mail: gemconference@gia.edu
Dr. James E. Shigley, Phone: 760-603-4019
Brendan M. Laurs, Phone: 760-603-4503
Fax: 760-603-4021
Web: www.gia.edu/gemsandgemology
or www.symposium.gia.edu